HHS Public Access

Author manuscript

Dev Biol. Author manuscript; available in PMC 2017 January 01.

Published in final edited form as:

Dev Biol. 2016 January 1; 409(1): 218–233. doi:10.1016/j.ydbio.2015.10.022.

Multiple Mouse Models of Primary Lymphedema Exhibit Distinct Defects in Lymphovenous Valve Development

Xin Geng[1], **Boksik Cha**[1], **Md. Riaj Mahamud**[1], **Kim-Chew Lim**[3], **Robert Silasi-Mansat**[1], **Mohammad K.M. Uddin**[4], **Naoyuki Miura**[4], **Lijun Xia**[1], **Alexander M. Simon**[5], **James Douglas Engel**[3], **Hong Chen**[1], **Florea Lupu**[1], and **R. Sathish Srinivasan**[1,2,*]

[1]Cardiovascular Biology Research Program, Oklahoma Medical Research Foundation, Oklahoma City, Oklahoma, USA

[2]Department of Cell Biology, University of Oklahoma Health Sciences Center, Oklahoma City, Oklahoma, USA

[3]Department of Cell and Developmental Biology, University of Michigan Medical School, Ann Arbor, Michigan, USA

[4]Department of Biochemistry, Hamamatsu University School of Medicine, Hamamatsu, Japan

[5]Department of Physiology, University of Arizona, Tucson, Arizona, USA

Abstract

Lymph is returned to the blood circulation exclusively via four lymphovenous valves (LVVs). Despite their vital importance, the architecture and development of LVVs is poorly understood. We analyzed the formation of LVVs at the molecular and ultrastructural levels during mouse embryogenesis and identified three critical steps. First, LVV-forming endothelial cells (LVV-ECs) differentiate from PROX1^{+} progenitors and delaminate from the luminal side of the veins. Second, LVV-ECs aggregate, align perpendicular to the direction of lymph flow and establish lympho-venous connections. Finally, LVVs mature with the recruitment of mural cells. LVV morphogenesis is disrupted in four different mouse models of primary lymphedema and the severity of LVV defects correlate with that of lymphedema. In summary, we have provided the first and the most comprehensive analysis of LVV development. Furthermore, our work suggests that aberrant LVVs contribute to lymphedema.

Introduction

Primary lymphedema is caused by mutations in genes that regulate normal lymphatic vascular development (Tammela and Alitalo 2010). Currently the only available treatments for this disease are palliative approaches like massage and compression. The primary

*Correspondence: sathish-srinivasan@omrf.org.

obstacle to advancing new therapies is the limited understanding of lymphatic vascular anatomy.

Lymphatic endothelial cells (LECs) are the building blocks of the entire lymphatic vasculature. Lymph collected by lymphatic capillaries is drained into collecting lymphatic vessels. Lymphatic valves within collecting vessels regulate the unidirectional flow of lymph. Collecting vessels then drain lymph into lymph sacs, which return it to the blood circulation via lymphovenous valves (LVVs) (Tammela and Alitalo 2010; Srinivasan and Oliver 2011). During this process, anchoring filaments regulate lymph uptake by capillaries, and perivascular cells that surround collecting lymphatic vessels regulate lymph propulsion (Tammela and Alitalo 2010). Lymphatic capillary hypoplasia, improper maturation of collecting lymphatic vessels and defects in lymphatic valves are all associated with primary lymphedema (Tammela and Alitalo 2010). However, there is limited information regarding other lymphatic anatomical structures such as LVVs, anchoring filaments and perivascular cells. Further, it is not known whether defects in any of these structures promote lymphedema (Chen et al. 2014).

We previously described several important anatomical and molecular characteristics of LVVs, which are the first valves to form within the lymphatic vasculature (Srinivasan and Oliver 2011). $PROX1^{+}$ cells are specified in the embryonic cardinal vein around E10 (Srinivasan et al. 2007). We showed that these cells have the capacity to differentiate into both LECs that migrate out from the veins to form the entire lymphatic vasculature or into LVV-forming endothelial cells (LVV-ECs) (Srinivasan and Oliver 2011). Mouse embryos that are haploinsufficient for the transcription factor PROX1 develop edema at E13.5, a stage at which lymphatic valves have not yet formed and LECs are only starting to sprout from lymph sacs (Srinivasan and Oliver 2011). At this stage, in addition to the dermal edema, the most conspicuous defect in $Prox1^{+/-}$ embryos is a lack of LVVs. This observation suggested that LVVs might be critical for proper lymphatic vascular functioning (Srinivasan and Oliver 2011). LVV defects have since been reported in mutant mice lacking integrin-α5 (ITGA5), CYP26B1 and GATA2, all of which develop severe edema and blood-filled lymphatics phenotypes (Bowles et al. 2014; Turner et al. 2014; Kazenwadel et al. 2015). LVVs are the only anatomical positions where lymph comes in direct contact with blood, and a recent report showed that platelets function at LVVs to regulate blood-lymphatic separation (Hess et al. 2014). Despite these findings, the key steps during LVV morphogenesis are not well characterized and there is no clear understanding of their three-dimensional architecture. The molecular mechanisms of LVV development are also not completely understood. This knowledge would likely facilitate the diagnosis and treatment of LVV defects.

Here, we employed a combination of fluorescence and electron microscopy approaches to characterize the structure and development of LVVs. By comparing LVVs with lymphatic valves and venous valves (VVs) we have identified similarities and also differences between these structures. Further, using four different murine models of lymphedema we show a strong correlation between defective LVVs and disease.

Results

Three-dimensional architecture of LVVs in newborn mice

We had previously described several key anatomical landmarks of lymphovenous valves (LVVs) in mouse embryos (Srinivasan and Oliver 2011). These landmarks are schematically shown in Supplementary Figure 1. Arteries and lymphatic valves are excluded from this figure for simplicity. A total of four LVVs are present in mice, with an “LVV-complex” containing two LVVs on either side of the body immediately lateral to the thymic lobules (orange structures). One of these locations is enlarged on the left to show the structures. The internal jugular vein, external jugular vein and subclavian vein merge together into the superior vena cava that drains deoxygenated blood into the right atrium of the heart. Venous valves (VV, depicted in green) guard the entry of veins into the junction. The lymph sac is split into two vessels by an artery just before entering the venous junction via LVVs (magenta). One LVV is located between the subclavian and external jugular veins. The other LVV is located between the external jugular vein and internal jugular vein. Using this information, we characterized the architecture of LVVs at the ultrastructural level.

We employed ProxTom lymphatic vessel reporter mice in correlative fluorescence and scanning electron microscopy (SEM) experiments. In these transgenic mice, the Prox1 promoter drives expression of the tdTomato (Tom) transgene, which encodes red fluorescent protein (Truman et al. 2012). We prepared cross sections encompassing the entire junction of veins, including the LVVs, from P0 ProxTom newborn mice (Supplementary Figure 1, between the dotted lines). We performed immunohistochemistry on these sections for the lymphatic endothelial cell (LEC) marker LYVE1 (lymphatic vessel endothelial hyaluronan receptor 1) and for the pan-endothelial cell marker CD31. Subsequently, we visualized the immunostained sections by confocal imaging in the anterior-to-posterior orientation (Ant) to observe the lymph sacs and the upstream side of LVVs. The samples were also analyzed in the posterior-to-anterior orientation (Pos) to observe the venous junction and the downstream side of LVVs and VVs en face.

In the Ant orientation, we observed weak Tom and LYVE1 expression in the LECs of the lymph sacs (Supplementary Figure 1 Ant, dotted lines). In contrast, we observed strong Tom expression in VV (Supplementary Figure 1 Ant, arrowhead) and LVVs (Supplementary Figure 1 Ant, white arrows). LYVE1 expression is absent in VVs, but is strongly expressed in LVVs (Supplementary Figure 1 Ant, white arrows). We also observed strong Tom and LYVE1 expressions in the lymphatic valve seen at the junction of a lymphatic vessel draining into the lymph sac (Supplementary Figure 1 Ant, red arrow). The scattered $LYVE1^{+}$ Tom^{-} cells are macrophages.

In the Pos orientation, the site of overlap between Tom^{+} cells and $LYVE1^{+}$ cells indicates the LVV, the entry point of the lymph sac into the vein (Supplementary Figure 1 Pos, white arrows). VVs and the lymphatic valve are also seen (Supplementary Figure 1 Pos, arrowheads and red arrow respectively).

After identifying the various anatomical structures by fluorescence microscopy as described above, the samples were carefully removed from the slides and processed for SEM. In the

Ant orientation, the lymph sacs appear positioned like a bird's nest at the branch point of the major veins (Figure 1A, pseudo colored in yellow). An artery is seen splitting the lymph sac into two lymphatic vessels. The upstream side of the LVVs is seen as narrow crevices in the middle of these vessels (Figure 1A, white and yellow arrows, the higher magnification picture of a LVV is pseudo colored in magenta). Cells at the entrance of LVVs appear elongated perpendicular to the direction of lymph flow (Figure 1A LVV, arrows). In comparison to LVVs, the VV at the entrance of the external jugular vein has a much wider opening (Figure 1A, pseudo colored in green). A higher magnification picture of this VV is also presented (Figure 1A VV). Cells upstream to the VV in the external jugular vein are rectangular in shape and appear to have aligned parallel to blood flow (Figure 1A VV, arrowheads and Supplementary Figure 2A). This is expected for endothelial cells exposed to laminar blood flow. Arterial endothelial cells are also aligned in the direction of blood flow (Supplementary Figure 2B). In contrast, cells on the upstream side of the VV have a round morphology (Figure 1A VV, arrows). Cells within the superior vena cava, downstream of VVs, also display a round morphology (Supplementary Figure 2A).

We were able to identify the downstream side of a lymphatic valve that is located at the entrance of a lymphatic vessel into lymph sacs (Figure 1A, red arrow). At higher magnification (Figure 1A LV, pseudo colored in blue), lymphatic valve cells are aligned perpendicular to the direction of fluid flow.

SEM in the Pos orientation revealed the downstream side of VV (Figure 1B, green) and LVVs (Figure 1B, magenta). VVs have longer leaflets compared to LVVs. At higher magnification, cells in the downstream side of VVs and LVVs appear elongated and perpendicular to the direction of fluid flow (Figure 1B, white and yellow arrowheads respectively). At the opening of the LVVs, we observe cloudy aggregates reminiscent of fibrin clots (Figure 1B, red arrowhead).

Unlike venous and lymphatic valves, each of which is composed of a homogeneous population of cells, LVVs are formed from a mixed population of endothelial cells: LECs from lymph sacs and the $PROX1^{+}LYVE1^{-}$ LVV-forming endothelial cells (LVV-ECs) from veins (Srinivasan and Oliver 2011). We performed transmission electron microscopy (TEM) using E18.5 embryos, which are developmentally very close to P0 pups, to visualize the interaction between LECs and LVV-ECs. In these sections LVV-ECs with distinct nuclei are seen on the outer side of the valve (Figure 1C, pseudo colored in magenta). However, very few nuclei are seen in the LECs (Figure 1C, pseudo colored in yellow). LECs appear to be profoundly stretched within LVVs. An extracellular matrix compartment is seen separating the LECs and LVV-ECs (Figure 1C).

In summary, LVVs share some similarities with VVs and lymphatic valves. Cells on the downstream side of these valves are elongated and arranged perpendicular to the direction of fluid flow. But, some important previously unanticipated differences exist. Most conspicuously, VVs have longer leaflets and larger opening compared to LVVs. And, cells at the upstream entrance of VVs appear cuboidal whereas the cells at the entrance of LVVs appear elongated.

Characterizing the stepwise morphogenesis of LVVs

Step I: LVV formation is initiated by the differentiation of LVV-ECs—Previous work revealed that LVV-ECs are not specified until E12.0 (Hagerling et al. 2011; Srinivasan and Oliver 2011). Therefore, we first analyzed E12.0 embryos to understand the characteristics of newly formed LVV-ECs. We prepared 12 μm frontal sections of the LVV-forming region from E12.0 wild-type embryos and analyzed them by immunohistochemistry using PROX1 and additional markers that were previously shown to be important for valve development (ITGA5, Integrin-α9 (ITGA9), FOXC2 and GATA2) (Petrova et al. 2004; Bazigou et al. 2009; Kazenwadel et al. 2012; Lim et al. 2012; Turner et al. 2014; Kazenwadel et al. 2015). Supplementary Figure 3 displays a schematic of the major veins and the LVV-forming region in E12.0 embryos. A magnified schematic of the LVV-forming region is shown in Figure 2A. These cartoons incorporate our findings, below. The results of our expression analyses for E12.0 and all subsequent stages are summarized in Figure 10.

At E12.0 external jugular vein and LVVs are located perpendicular to the internal jugular vein and superior vena cava. Based on the expression of valve markers we observed the earliest LVV rudiments at this stage (Figure 2B-E and Supplementary Figure 4). LVV-ECs have not yet invaginated into the vein. We were unable to identify any direct connection between the vein and lymph sac in E12.0 embryos, suggesting that lymphatic drainage has not yet begun. Consistent with other reports, we observed blood cells within lymph sacs of E12.0 embryos (Figure 2B, arrowheads) (Francois et al. 2012). Expression of PROX1, FOXC2 and GATA2 are significantly higher in LVV-ECs compared to LECs and the remaining PROX1$^+$ LEC progenitors on the vein. PROX1 expression in the LVV-ECs is 5-fold higher than that in the LEC progenitors on the vein and 1.5-fold higher than that in the LECs. FOXC2 expression in the LVV-ECs is 3.3-fold higher than that in the LEC progenitors and 9.5-fold higher than that in the LECs. Similarly, GATA2 expression in the LVV-ECs is 2.9-fold higher than that in the LEC progenitors and 4.6-fold higher than that in the LECs. Expressions of ITGA9 and ITGA5 also appear to be upregulated in the LVV rudiments (Figure 2 and Supplementary Figures 4, 5). The pan-endothelial cell junctional molecule CD31 also appears to be expressed at higher levels in LVV-ECs compared to LECs of the lymph sacs. In contrast, no obvious differences were observed in the expression of LYVE1 between LECs and LVV-ECs. Podoplanin (PDPN), which regulates blood-lymphatic separation (Fu et al. 2008; Bertozzi et al. 2010; Uhrin et al. 2010; Hess et al. 2014), is expressed in the LECs, but not in LVV-ECs. VEGFR3, the cognate receptor tyrosine kinase for lymphangiogeneic growth factor VEGFC (Tammela and Alitalo 2010), is expressed in all LECs and appears to be weakly expressed in LVV-ECs. VEGFR3 expression also appears to be increased in the LECs that are in close proximity to LVV-ECs. Furthermore, we observed only one Ki67$^+$ cells among 125 LVV-ECs from 3 embryos that we analyzed. In contrast, 64% (230 out of 357) of LECs in the nearby lymph sacs are Ki67$^+$. This result suggests that cell proliferation does not accompany LVV-EC differentiation (Supplementary Figure 5).

Next, we wanted to visualize the LVV-ECs at high resolution using SEM. Based on our findings above, we reasoned that LVV-EC clusters are best-visualized en face in sagittal sections. Indeed, confocal imaging of sagittal sections of ProxTom embryos co-

immunostained for CD31 and VEGFR3 revealed two loose clusters of Tom^{high};$VEGFR3^{+}$;$CD31^{+}$ cells (Figure 2F, arrows). The artery that is normally seen in between the two LVVs at P0 is also observed at this stage (Figure 2F, dotted lines). We used the same section to perform SEM as described above (Figure 2F). SEM revealed individual LVV-ECs with squamous morphology delaminating from the wall of the vein (Figure 2F, pseudo colored in magenta). These delaminating LVV-ECs aggregate one on top of another with numerous filopodia-like projections, suggestive of cell migration.

Some variability is observed in the development of LVVs. A few (2 out of 8 embryos analyzed) E12.0 embryos have only formed the anterior LVV-EC cluster, suggesting that this cluster forms earlier than the posterior cluster. SEM of this cluster also revealed structures indicative of active cell migration (Supplementary Figure 6). Cells in the region where the second LVV-EC cluster would form have not yet upregulated Tom expression and remain flat like the rest of the venous endothelium. In summary, the above results indicate that LVV-ECs, and the LECs that are in their vicinity, have a distinct molecular identity at E12.0.

With this knowledge we next analyzed E11.5 embryos to gain a better understanding about the progenitors that give rise to LVV-ECs. We prepared 12 μm frontal sections of E11.5 embryos in the dorsal to ventral orientation and analyzed them as described above. As expected we did not observe ITGA9 expression in the $PROX1^{+}$ cells on the vein (Supplementary Figure 7A-C). In contrast, PROX1, FOXC2 and GATA2 showed heterogeneous expression pattern. PROX1 expression is significantly enriched in the LECs located outside the cardinal vein and in the LEC progenitors located dorsally on the cardinal vein (Supplementary Figure 7, arrows). Francois et al named these progenitor cells as the pre-lymphatic cluster (PLC) (Francois et al. 2012). An artery is observed at a posterior and ventral position with respect to the PLC (Supplementary Figure 7, yellow arrows). Based on this landmark we speculate that the progenitors of LVV-EC are located in the cardinal vein at this vicinity (Supplementary Figure 7, dotted lines). Interestingly, PROX1 expression is much weaker in these cells in comparison to LECs and the dorsal LEC progenitors (Supplementary Figure 7A-H). Little or no significant differences are observed in the expression of FOXC2 and GATA2 within the $PROX1^{+}$ cells on the vein (Supplementary Figure 7C-G, I, J). However, both FOXC2 and GATA2 are significantly downregulated in LECs. In summary, these results confirm that LVV-EC differentiation has not occurred at E11.5.

Step II: LVV-ECs aggregate and elongate to form LVVs—At E12.5, approximately 12 hrs after the differentiation of LVV-ECs, the external jugular vein has rotated clockwise by 45° towards internal jugular vein (Supplementary Figure 3 and Figure 3A). We observed at least one open connection between the lymph sacs and veins via the LVV (Figure 3B, red arrow). Blood cells are rarely observed in lymph sacs at E12.5. Immunohistochemistry on frontal sections of E12.5 embryos revealed that the expression patterns of PROX1, PDPN, VEGFR3, FOXC2, GATA2 and ITGA9 are similar to E12.0 (Figure 3B and data not shown). VEGFR3 expression appears to be higher in the LECs that are close to LVV-ECs, and the expression of ITGA9 appears to be higher at the interface of LECs and LVV-ECs.

LYVE1 is expressed in LECs and in some venous endothelial cells, but is specifically excluded from LVV-ECs.

Next we investigated E12.5 ProxTom embryos by correlative fluorescence microscopy and SEM, as described above. We prepared sagittal sections of embryos, co-immunostained for VEGFR3 and CD31, and imaged them together with Tom. Confocal microscopy revealed that the Tom^{high} cells have aggregated into more compact and clearly distinct clusters (Figure 3C). SEM on the same samples revealed that LVV-ECs have assumed an elongated morphology perpendicular to the direction of blood flow (Figure 3C and Supplementary Figure 8). Very few filopodia-like projections, if any, were observed suggesting that the cells are not migratory.

Step III: LVVs undergo gradual maturation with the recruitment and differentiation of mural cells—By E14.5 the remodeling of veins has ceased and the overall arrangement of major veins is similar to that described above for P0 newborn mice (Figure 1). The external jugular vein has rotated further clockwise towards the midline. External and internal jugular veins are almost parallel to each other and to the superior vena cava. The LVVs are now positioned vertically above the junction of jugular and subclavian veins. After E14.5 the most conspicuous change in this lymphovenous junction is the development of VVs, which become clearly visible at E16.5. A schematic representation of this region in the frontal orientation at E16.5 is presented Supplementary Figure 3 and in Figure 4A.

We collected E14.5, E16.5 and E18.5 embryos and evaluated the expression of various LEC and LVV-EC markers by immunohistochemistry. PROX1, CD31 and the valve markers GATA2, FOXC2, ITGA9 and ITGA5 are strongly expressed in LVVs and VVs at these stages (Supplementary Figure 9). At E14.5, VEGFR3 and PDPN are strongly expressed in LECs within the lymph sac and LVV (Figure 4B). As before, VEGFR3 expression appears to be stronger in LECs that are in close proximity to LVV-ECs. After E14.5 we observed a gradual reduction in the expression of PROX1, VEGFR3 and PDPN in the LECs of lymph sacs. However, these LEC markers remain strongly expressed within LVVs at all time points (Figure 4B, arrows). The downregulation of LEC markers in collecting lymphatic vessels is known to coincide with the recruitment of mural cells (Makinen et al. 2005). Thus, we evaluated the expression of LYVE1 together with mural cell markers PDGFRβ, smooth muscle α-actin (SMA), smooth muscle cell-myosin heavy chain 11 (MYH11) and NG2 by immunofluorescence (Figure 5). PDGFRβ is considered as the earliest marker for the entire mural cell lineage (Armulik et al. 2011). SMA and MYH11 are markers for a subset of mural cells known as vascular smooth muscle cells (Majesky et al. 2011). NG2 is a marker for another subset of mural cells known as pericytes (Armulik et al. 2011).

Similar to VEGFR3 and PDPN, a gradual downregulation of LYVE1 in lymph sacs is observed between E14.5 and E18.5 (Figure 5). At E14.5 several $PDGFR\beta^+$ cells are seen surrounding the lymph sacs (Figure 5A, red arrowheads). A few $PDGFR\beta^+$ cells are also seen in the LVVs (Figure 5A, arrows). However, these cells do not express SMA, MYH11 or NG2 (Figure 5D, G, J) suggesting that the $PDGFR\beta^+$ cells are undifferentiated mesenchymal progenitors.

At E16.5, the only obvious change in the expression of PDGFRβ is its presence in VVs (Figure 5B, white arrowheads). However, at this stage numerous SMA^+, $MYH11^+$ and $NG2^+$ cells are seen in the lymph sacs, LVVs and VVs suggesting that these are differentiated mural cells (Figure 5E, H, K, red arrowheads, white arrows and white arrowheads respectively).

At E18.5 the expression pattern of all mural cell markers within LVVs and VVs is similar to that at E16.5 (Figure 5C, F, I, L, white arrows and white arrowheads respectively). In the lymph sac, expression of PDGFRβ and MYH11 is comparable to that at E16.5 (Figure 5C, I, red arrowheads). In contrast SMA^+ cells have increased in lymph sacs (Figure 5F, red arrowheads). And, due to a tremendous increase in the expression of NG2 in the mesenchymal compartment we are unable to conclusively determine whether this marker is increased in the mural cells surrounding the lymph sacs (Figure 5L).

We confirmed the presence of interstitial cells within the LVV by TEM (Supplementary Figure 10, pseudo colored in brown). The presence of enlarged secretory endoplasmic reticulum (Supplementary Figure 10, arrows) suggest that these are cells with mural/myofibroblast-like characteristics that produce extra cellular matrix components (Phan 2002).

In summary, we have determined that mesenchymal cells are recruited to lymph sacs and LVVs. The maturation of lymph sacs into a collecting lymphatic vessel-like structure is associated with the differentiation of mesenchymal cells into mural cells. To the best of our knowledge mural cells have not been reported so far in lymphatic or venous valves. In fact, lymphatic valves were shown to lack SMA^+ cell coverage and precocious mural cell recruitment was suggested to inhibit lymphatic vessel maturation (Petrova et al. 2004). However, a recent publication reported the occasional presence of cells with fibroblast-like characteristics within the lymphatic valves (Kanady et al. 2011). Whether they are similar to the mural cells observed in LVVs and VVs remains to be determined.

To analyze LVV-ECs at higher resolution, we prepared transverse sections from E14.5, E16.5 and E18.5 ProxTom embryos. These sections were analyzed by confocal fluorescence microscopy followed by SEM in the Pos orientation (Figure 6). We identified LVVs using both approaches (Figure 6A-C, arrows and 6D-F, pseudo colored in magenta), and observed only subtle changes during this time interval. LVVs do not invaginate further into veins. However, LVV-ECs become thinner and more elongated (Figure 6D-F). We propose that LVV-ECs are stretched due to the overall increase in the diameter of veins during this time window. Whether the mural cells recruited to the valves during this interval play any role in this morphogenetic process is not known.

During this same E14.5-E18.5 time window, VVs undergo dramatic morphogenesis near LVVs (Figure 6A-C, arrowheads and 6D-F, pseudo colored in green). At E14.5 VVs are not observed; however, several layers of cells can be seen delaminating at the rim of the veins (Supplementary Figure 11A-C). This likely corresponds to stages 0–1 of VV development, as previously described by Bazigou et al (Bazigou et al. 2011). At E16.5 the VV at the entrance to the internal jugular vein appears as a circular shelf (Figure 6E, red arrowhead),

corresponding to stage 2 of VV development (Bazigou et al. 2011). The VV at the entrance of the external jugular vein appears with a commissure and corresponds to stage 3 (Figure 6E, white arrowhead) (Bazigou et al. 2011). By E18.5, the VV at the entrance of the external jugular vein is in stage 4 of its development and has a dome shaped structure (Figure 6F) (Bazigou et al. 2011). Cell shape changes accompany VV morphogenesis as well. At E14.5 delaminating cells appear round because of the clearly visible cell body (Supplementary Figure 11B, C). At E16.5 cells at the tip of VVs are elongated (Supplementary Figure 11D, arrowheads). In contrast, cells lying underneath on the downstream side of VVs are round (Supplementary Figure 11D, arrows). By E18.5 and at P0 all of the cells on the downstream side of VVs are elongated (Supplementary Figure 11E, F, arrows). Thus, although VVs and LVVs express similar genes at this stage of development, their structure and morphology are quite distinct. Specifically, VVs add multiple layers of cells and are wide open, whereas LVVs are compact and contain fewer cells (Figure 6F).

LVVs are defective in multiple mouse models of primary lymphedema Having characterized the stepwise development of LVVs, we asked if LVVs are defective in mouse models of primary lymphedema.

Prox1: As described above, PROX1 expression is enriched in LVV-ECs. The increased expression of PROX1 in restricted cells within the vein at E12.0 is the first clear sign that LVV morphogenesis has begun. We previously showed that Prox1 dosage is critical for the differentiation of LVV-ECs and for the development of LVVs (Srinivasan and Oliver 2011). We first wanted to recapitulate these findings using our confocal and SEM approaches. We sectioned wild-type ProxTom and ProxTom;Prox1$^{+/-}$ E16.5 embryos. We immunostained these sections for LYVE1 and CD31, followed by confocal imaging in the Ant and Pos orientations as described in Supplementary Figure 1. In the Ant orientation, the lymph sacs of ProxTom;Prox1$^{+/-}$ embryos are much smaller compared to that of wild-type control littermates (Supplementary Figure 12A, B). Additionally, LECs from ProxTom;Prox1$^{+/-}$ embryos express higher levels of LYVE1 than their control littermates, implying a defect in lymph sac maturation. Formation of VV at the entrance of external jugular vein is arrested in the mutants (Supplementary Figure 12A, B, arrowheads). In the Pos orientation, LVVs, where LYVE1^{+} LECs intersect with LYVE1^{-} LVV-ECs, are clearly present in control embryos (Supplementary Figure 12C, arrows). Nearby VVs are also observed (Supplementary Figure 12C, arrowheads). Tom expression is enriched in both LVVs and VVs. In contrast, Tom expression was much weaker in a similar section from ProxTom;Prox1$^{+/-}$ embryos, and a connection between lymphatic vessels and vein was not observed (Supplementary Figure 12D). VV at the entrance of internal jugular vein is absent in Prox1-heterozygotes.

We analyzed eight LVV-complexes from E16.5 ProxTom;Prox1$^{+/-}$ and wild-type ProxTom embryos by SEM. Again, we observed LVVs and VVs in control embryos but not in Prox1$^{+/-}$ embryos (Supplementary Figure 12E, F). Identical results were obtained from seven samples. In one sample we observed a valve-like opening, although it is much smaller than the LVVs seen in control embryos (data not shown).

In conclusion, the analyses of Prox1$^{+/-}$ embryos by confocal imaging and by SEM validated our previous finding that these embryos lack LVVs. Our analysis has also revealed an additional previously unknown defect (lymph sac maturation) in Prox1$^{+/-}$ embryos.

Foxc2: FOXC2 is necessary for the maturation of collecting lymphatic vessels and for the formation of lymphatic valves therein (Petrova et al. 2004). To determine if FOXC2 is also necessary for the development of LVVs, and to test the hypothesis that a defect in LVVs could contribute to lymphedema, we generated Foxc2$^{+/-}$ mice in which one Foxc2 allele is replaced with the cDNA for CreERT2 (please see Methods for more details). In C57BL/6 background we observed a variable phenotype in Foxc2$^{+/-}$ embryos. Approximately 50% of Foxc2$^{+/-}$ embryos develop severe edema by E14.5, whereas the remaining heterozygous embryos were grossly normal (Figure 7A-C). At this stage, lymph sacs and LVVs are present, but collecting lymphatic vessel maturation has not taken place and lymphatic valves are not yet formed (Norrmen et al. 2009). We were able to identify LVV-ECs and LVVs in normal-looking, but not in edematous, Foxc2$^{+/-}$ E14.5 embryos by immunohistochemistry (Figure 7D-F). However, normal-looking Foxc2$^{+/-}$ embryos contain only one LVV compared to two in the LVV-complex of wild-type control embryos. We confirmed these results by performing SEM using 3 wildtype, 4 normal-looking Foxc2$^{+/-}$ and 2 edematous Foxc2$^{+/-}$ embryos (Figure 7G-I). Thus, the edematous phenotype correlates with the LVV defect.

We next analyzed E14.5 wild-type control and Foxc2$^{-/-}$ homozygous embryos. We found that Foxc2$^{-/-}$ null embryos are edematous and their lymph sacs are dilated (Supplementary Figure 13A, B). Although Prox1^{+} LVV-ECs are observed in Foxc2$^{+/+}$ wild-type embryos, these cells are completely absent in Foxc2$^{-/-}$ null embryos. We obtained identical results with a previously reported Foxc2 knockout model (data not shown) (Iida et al. 1997).

Connexin37: The gap junction molecule Connexin37 (Cx37) is a putative target gene of the transcription factor FOXC2 and is expressed in lymphatic valves and VVs (Kanady et al. 2011; Sabine et al. 2012). Cx37$^{-/-}$ null mice display dilated lymph sacs and lymph reflux, indicating that this target is required for proper development and lymphatic function (Kanady et al. 2011). Lymphatic valve-forming cells are specified in Cx37$^{-/-}$ embryos (Sabine et al. 2012); however, most of these cells do not undergo proper morphogenesis into mature lymphatic valves (Kanady et al. 2011; Sabine et al. 2012). Indeed, very few lymphatic valves are observed in the mesenteric lymphatic vessels of Cx37$^{-/-}$ embryos (Kanady et al. 2011). We wanted to determine if CX37 is necessary for LVV-EC differentiation. We found that CX37 is expressed in both LECs and LVV-ECs by immunohistochemistry in E16.5 wild-type embryos (Supplementary Figure 14). We next analyzed the LVV-forming region in E16.5 Cx37$^{-/-}$ embryos. The expression of PROX1, FOXC2, VEGFR3 and ITGA9 are not affected in the LVV-ECs of Cx37$^{-/-}$ embryos (Figure 8 and data not shown). However, LVV-ECs do not invaginate into the veins in these mutant embryos. Thus, although CX37 is not required for LVV-EC differentiation, it is required for their proper morphogenesis. Furthermore, FOXC2 plays a CX37 independent role in specifying LVV-ECs.

Gata2: Mutations in GATA2 cause Emberger syndrome and the carriers are predisposed to leukemia and lymphedema (Ostergaard et al. 2011; Kazenwadel et al. 2012). GATA2 expression in mice is enriched in lymphatic valves (Kazenwadel et al. 2012). As shown above, GATA2 is expressed in LVV-ECs from the earliest developmental time point. Based on these data, we wanted to determine if GATA2 is required for the formation of LVVs. We were unable to analyze LVVs in $Gata2^{-/-}$ embryos since they die prior to LVV formation, at E10 (Tsai et al. 1994; Khandekar et al. 2007). Therefore, we took a time-specific deletion approach to overcome the early lethality of $Gata2^{-/-}$ embryos. A transgenic vascular endothelial cell-specific, tamoxifen-inducible CreERT2 line (Tg^{VE}) was recently reported (Lim et al. 2012). This line was generated using an endothelial cell-specific regulatory element of Gata2 (Khandekar et al. 2007). Using VE-mCherry we determined that this regulatory element is active in both LECs and LVV-ECs. Additionally, by lineage tracing we determined that Tg^{VE} is active in both LECs and LVV-ECs (Supplementary Figure 15). Conditional deletion of Gata2 using Tg^{VE} resulted in severe lymphedema and blood-filled lymphatics (Lim et al. 2012). We analyzed sections from E13.5 Tg^{VE};$Gata2^{f/-}$ embryos treated with tamoxifen at E10, and from control E13.5 $Gata2^{+/-}$ heterozygous embryos. We found that Tg^{VE};$Gata2^{f/-}$ embryos display reduced PROX1 expression within the LVV-forming region compared to control embryos (Figure 9A-D, arrows). The expression of the LVV-EC markers FOXC2, VEGFR3 and ITGA9 are also reduced or eliminated in the LVV-forming region of Tg^{VE};$Gata2^{f/-}$ embryos relative to control embryos (Figure 9C-F, arrows and data not shown). We conclude that properly differentiated LVV-ECs are absent in Tg^{VE};$Gata2^{f/-}$ embryos, a result that is consistent with a recent report (Kazenwadel et al. 2015).

In conclusion, LVVs are defective in multiple models of primary lymphedema. Importantly, phenotypically obvious lymphedema correlates with the complete absence/deformation of LVVs.

Discussion

Lymph is returned to the blood circulation exclusively via LVVs, which are the first valves to form within the lymphatic vasculature. Large volume of lymph (1–2 liters) pass through LVVs everyday in average human adults (Tammela and Alitalo 2010). LVVs also prevent blood from entering the lymphatic vessels (Hess et al. 2014). Due to their strategic location, time of formation, and functional significance, we wanted to understand their structure and role in lymphatic vascular functioning. We characterized the development of LVVs using innovative imaging techniques and clinically relevant mouse models. We present the first and the most comprehensive information about the molecular and structural events during LVV morphogenesis. Our work suggests that defects in LVV contribute to lymphedema. Here we discuss some novel insights about the morphogenesis of LVVs. We also highlight some unanswered questions and therapeutic opportunities.

Stepwise morphogenesis of LVVs—Our data support a three-step developmental mechanism for LVVs (Figure 10). By using mutant models we have gained insights into the molecular mechanisms that are operating in each of these steps.

Step I: Delamination of LVV-ECs—At E12.0 LVV-ECs delaminate from veins as loose clusters of cells. Based on our observations, we hypothesize that two closely related processes generate LVV-ECs. First, $PROX1^+$ progenitors are specified in the LVV-forming region of the vein. SOX18, COUP-TFII and PROX1 are necessary progenitor specification (Wigle and Oliver 1999; Francois et al. 2008; Srinivasan et al. 2010; Srinivasan and Oliver 2011). Second, PROX1, FOXC2 and GATA2 are upregulated in these progenitors, leading to their differentiation into LVV-ECs.

PROX1 overexpression in cultured blood endothelial cells reprograms them into LECs (Hong et al. 2002; Petrova et al. 2002; Srinivasan et al. 2014). Then why do some $PROX1^+$ progenitors differentiate into LVV-ECs and not LECs? The $PROX1^+$ cells on the cardinal vein are undifferentiated progenitors. We previously demonstrated that these progenitors at E10.5 have the capacity to differentiate into both LVV-ECs and LECs (Srinivasan and Oliver 2011). Existing data suggests that VEGFC regulates the migration of cells from the vein to cause their differentiation into LECs (Karkkainen et al. 2004). In contrast, oscillatory fluid flow might be controlling the differentiation of progenitors into LVV-ECs (Sabine et al. 2012). We speculate that the progenitors that give rise to LVV-ECs are located more ventrally in the cardinal vein in comparison to those that give rise to LECs (Supplementary Figure 7). It is possible that the dorsal and ventral progenitor populations are differentially exposed to the two lineage-determining signals.

The delamination of LVV-ECs into the lumen of vein is reminiscent of the endothelial to mesenchymal transition that occurs during cardiac valve formation (Armstrong and Bischoff 2004). Interestingly, FOXC2 and its cofactor NFATC1 are both necessary for cardiac valve formation (Chang et al. 2004; Seo and Kume 2006; Norrmen et al. 2009). Whether FOXC2 plays a role in the delamination of LVV-ECs remains to be tested. Nevertheless, based on the observed phenotype of $Cx37^{-/-}$ embryos we speculate that Cx37, a target of FOXC2, is necessary for this step.

Step II: Organization of LVV-ECs into LVVs—Next, LVV-ECs elongate, interact with each other and organize themselves perpendicular to blood flow. The signals that regulate these steps are currently not known. Such highly coordinated cell behaviors most likely involve specialized pathways. Planer cell polarity is one such pathway that was recently reported to operate during lymphatic valve development (Tatin et al. 2013). Molecules involved in cytoskeletal organization such as Rho, Rac and Cdc42 might play important roles in this process.

Step III: Maturation of LVVs—Interstitial cells with mural cell characteristic are present in cardiac valves and are thought to play important role in matrix secretion, cell-cell communication, wound repair and contractility. Such SMA^+ cells are absent from lymphatic valves (Petrova et al. 2004). Here we have shown that between E14.5 and P0, LVVs mature with the recruitment of mural cells into the valve leaflets. This coincides with the maturation of lymph sacs into a collecting lymphatic vessel-like structure. On the left side of the body, the mature lymph sac connects with the thoracic duct, the largest collecting vessel of the body. The collecting vessel on the right side likely drains lymph from the lungs (para tracheal lymph plexus) and the upper right side of the body. The recruitment of mural cells

is likely critical for the proper morphogenesis and functioning of LVVs and could involve the interplay of factors such as PDGFB, ANG1, ANG2 and their cognate receptors (Adams and Alitalo 2007). In the future it will be important to determine if mutations in these factors abrogate LVV formation or functioning.

We found that $Prox1^{+/-}$ embryos have smaller lymph sacs that do not mature properly. This phenotype may arise from a direct role of PROX1 in the LECs, or indirectly from a defect in the lymph flow caused by the absence of LVVs. Alternatively, a critical mass of LECs may have to be present in lymph sacs before they differentiate.

Similarities and differences between LVVs and other valves—Work from the labs of Tatiana Petrova and Taija Makinen have provided important insights into the development of VVs and LVs. Their work suggests that VVs and LVs are largely similar in their molecular profile and developmental characteristics (Bazigou et al. 2011). LVVs form in close proximity to the earliest VVs that form within jugular and subclavian veins. By comparing LVVs with the nearby VVs we have identified both similarities and differences between them.

LVVs have a much smaller opening compared to VVs and lymph valves (Figure 1). Second, the morphogenesis of LVVs is unique. LVV-ECs are specified before lymphatic drainage into veins is initiated. Newly specified LVV-ECs inside the vein and LECs that are outside the vein undergo a series of coordinated remodeling steps to form LVVs and establish a connection between blood and lymphatic vessels. In contrast, VVs and lymphatic valves are each composed of one cell type and form within vessels in which fluid flow is already taking place.

Despite such major differences, LVVs express the same set of markers as VVs and lymph valves. In fact, in most of our mouse models of primary lymphedema, both VV and LVV development are defective, highlighting the conservation of some basic developmental mechanisms. Our work also clarifies some controversies regarding valve development. Sabine et al. reported that fluid flow triggers the differentiation of lymphatic valve-forming cells by promoting a rounded morphology in LECs (Sabine et al. 2012). In contrast, Tatin et al. suggested that elongation of LECs is the first step of lymphatic valve development (Tatin et al. 2013). We have found that LVV-ECs are transiently squamous at the time of their delamination from veins (Figure 2F). Shortly afterwards, LVV-ECs have a large cell body and an elongated cytoplasm (Supplementary Figure 8). VV-forming cells also have a similar morphology at the beginning of valve morphogenesis (Supplementary Figure 11). Therefore, at this stage valve-forming cells could be called cuboidal or elongated depending on whether a nuclear (i.e. Sabine et al.) or cytoplasmic (i.e. Tatin et al.) marker is used to visualize them. However, considering the morphology of the entire cell, it is more appropriate to state that the valve-forming cells are elongated at this stage.

Clinical relevance—We have identified LVV defects in four different mouse models of primary lymphedema. LVVs are the first anatomical structures to form within the lymphatic vasculature after the differentiation of LECs. All of the presented mouse models develop obvious edema by E14.5, prior to the formation of lymphatic valves and the maturation of

collecting lymphatic vessels. The only obvious defects we could identify were the LVV defects. So, while LVVs may not be sufficient for lymphatic vascular functioning (Coxam et al. 2014; Klein et al. 2014; Outeda et al. 2014), our data suggest that defective LVVs are incompatible with normal lymphatic physiology.

Indeed, analyzing LVV structure is likely to have prognostic value in predicting lymphedema. Based on our findings it is tempting to speculate that human primary lymphedema patients (with mutations in FOXC2 or GATA2) are born with abnormal LVVs. These patients have sufficient lymphatic vascular function until LVV function falls below a critical threshold, triggering the onset of disease. The capacity to identify these subtle defects in LVVs by non-invasive approaches could be powerful in predicting the likelihood of developing lymphedema. Correcting LVV defects in a timely manner might prevent the progression of lymphedema. It appears to be technically feasible to locate LVVs (Seeger et al. 2009); whether such approaches could evolve to detect subtle LVV defects remains to be seen. We observe both LVV and VV defects in most of our mouse models of lymphedema. Therefore, identifying VV defects might play a surrogate role in predicting LVV defects.

In conclusion, we have provided novel information regarding the morphogenesis of LVVs at high resolution. We hope that our findings will provide the necessary structural and molecular framework to facilitate the diagnosis of LVV defects and to assist in developing strategies to repair those defects.

Methods

Mouse models—ProxTom, Prox1$^{+/GFPCre}$ (Prox1$^{+/-}$), Foxc2$^{+/-}$, Gata2$^{+/-}$, Tg^{VE};Gata2$^{f/f}$ and Cx37$^{+/-}$ mice were reported previously (Tsai et al. 1994; Iida et al. 1997; Simon et al. 1997; Srinivasan et al. 2010; Lim et al. 2012; Truman et al. 2012). We generated a new Foxc2$^{+/CreERT2}$ mouse line by replacing the open reading frame of Foxc2 with a cDNA for CreERT2 (Cyagen Biosciences, Santa Clara, CA, USA). The 5` and 3` UTR's were kept intact. Standard Southern Blot and PCR approaches verified proper targeting to the Foxc2 locus. The neomycin selection cassette was flanked by FLP sites and was removed by breeding the properly targeted mice with R26-Flpase mice (Jax Stock number 009086) (Raymond and Soriano 2007). Immunohistochemistry on Foxc2$^{CreERT2/CreERT2}$ samples with anti-FOXC2 antibody (see below) further confirmed proper targeting and deletion of Foxc2. All mice were housed and handled according to the institutional IACUC protocols.

Immunohistochemistry—For vibratome sections, embryos were fixed in 4% paraformaldehyde (PFA) at 4°C overnight (E12.0 to E14.5) or for 72 hours (E16.5 and E18.5). After washing several times in PBS embryos were embedded in 7% low melting point agarose (Life technologies, Grand Island, NY, USA), and 500 or 800 μm sections were prepared using vibratome (Leica, Buffalo Grove, IL, USA) and immunostained as described previously (Yang et al. 2012). The sections were mounted with polyvinyl alcohol mounting medium with DABCO (Sigma-Aldrich, St. Louis, MO, USA) and then visualized with a LSM 710 confocal laser-scanning microscope (Zeiss, Oberkochen, Germany). Subsequently, 3-D confocal stacks were reconstructed using Imaris 7.7.1 software (Bitplane, Zurich, Switzerland).

For cryosections, embryos were fixed in 4% PFA as described above and embedded in Tissue-tek O.C.T (Sakura, Alphen aan den Rijn, The Netherlands). 12 μm sections were prepared using cryotome and immunohistochemistry was carried out as described previously. For Cx37 staining, unfixed embryos were quick frozen in O.C.T and 12 μm sections were prepared using cryotome. Immunostaining for Cx37 was described previously (Kanady et al. 2011; Munger et al. 2013). After mounting, the sections were visualized with Eclipse 80i microscope (Nikon, Tokyo, Japan) equipped with Zyla sCMOS camera (Andor Technology, Belfast, UK) and analyzed using NIS-Elements BR software (Nikon, Tokyo, Japan). Semi-quantitative measurement of fluorescent signal intensity was carried out using ImageJ (NIH, Bethesda, USA) as described recently (Potapova et al. 2011). Briefly, the regions of interest (the nuclei of cells) were individually selected and the mean intensity was measured after background correction. Statistical significance was measured using GraphPad Prism (GraphPad Software Inc, San Diego, USA).

Antibodies—Primary antibodies used for immunostaining were as follows: rabbit anti-PROX1 (AngioBio, San Diego, CA, USA); goat anti-human PROX1 (R&D Systems, Minneapolis, MN, USA); rat anti-mouse FOXC2 (Furumoto et al. 1999); goat anti-mouse VEGFR3 (R&D Systems, Minneapolis, MN, USA); hamster anti-mouse podoplanin (Biolegend, San Diego, CA, USA); goat anti-mouse LYVE1 (R&D Systems, Minneapolis, MN, USA); rat anti-mouse CD31 (BD Pharmingen, San Jose, CA, USA); goat anti-mouse ITGA9 (R&D Systems, Minneapolis, MN, USA); rat anti-mouse ITGA5 (BD Pharmingen, San Jose, CA, USA); goat anti-mouse GATA2 (R&D Systems, Minneapolis, MN, USA); rabbit anti-mouse CX37 (Life technologies, Grand Island, NY, USA); rabbit anti-bovine MYH11 (Biomedical Technologies Inc, Stoughton, MA, USA); goat anti-mouse PDGFRβ (R&D Systems, Minneapolis, MN, USA): Cy3-conjugated monoclonal anti-SMA (Sigma-Aldrich, St. Louis, MO, USA); and rabbit anti-rat NG2 (EMD Millipore, Billerica, MA, USA). The following secondary antibodies were used: Cy3-conjugated donkey anti-rabbit (Jackson ImmunoResearch Laboratories, West Grove, PA, USA); Cy5-conjugated donkey anti-rat (Jackson ImmunoResearch Laboratories, West Grove, PA, USA); Alexa 488-conjugated donkey anti-goat (Life technologies, Grand Island, NY, USA); Alexa 488-conjugated goat anti-chicken (Life technologies, Grand Island, NY, USA); Alexa 488-conjugated donkey anti-rat (Life technologies, Grand Island, NY, USA); Alexa 647-conjugated goat anti-hamster (Life technologies, Grand Island, NY, USA).

Transmission Electron Microscopy—E18.5 mouse embryos were fixed in a mixture of 2% PFA and 2.5% glutaraldehyde in 0.1 M sodium cacodylate buffer at 4°C for 2 days. The fixed embryos were processed for vibratome section as described above. 1 mm thick sections that contain the LVV-complex were collected and trimmed into 1 mm cubes to remove other tissues regions. The samples were post-fixed in 1% osmium tetroxide for 90 minutes and 1% tannic acid for 1 hour. The samples were subsequently dehydrated gradually in increasing concentrations of ethanol and embedded in epoxy resin (Electron Microscopy Sciences, Hatfield, PA, USA). Semi-thin (500 nm) and ultra-thin (70 nm) sections were obtained using an ultramicrotome (RMCMT-7000, Boeckler Instruments Inc, Tuscon, AZ, USA) equipped with a diamond knife. Semi-thin sections were stained with Epoxy tissue stain (Electron Microscopy Sciences, Hatfield, PA, USA) and analyzed with a

Eclipse E800M microscope (Nikon, Tokyo, Japan). Ultrathin sections were stained with uranyl acetate and lead citrate before being viewed with a Hitachi H-7600 electron microscope equipped with a 4 megapixel digital monochrome camera and AMT-EM image acquisition software (Advanced Microscopy Techniques, Danvers, MA, USA).

Scanning Electron Microscopy—Both freshly prepared vibratome sections or those used for immunohistochemistry and confocal microscopy analyses were fixed in 2% glutaraldehyde in 0.1 M cacodylate buffer for 2 hours. After washing profusely in PBS, the sections were post fixed in 1% osmium tetroxide in 0.1 M cacodylate buffer for 2 hours and subsequently dehydrated in a graded ethanol series. The sections were further dehydrated in hexamethldisilazane (HMDS) and allowed to air-dry overnight. Dry sections were sputter-coated with Au/Pd particles (Med-010 Sputter Coater by Balzers-Union, USA) and observed under Quanta SEM (FEI, Hillsboro, OR, USA) at an accelerating voltage of 20KV.

Supplementary Material

Refer to Web version on PubMed Central for supplementary material.

Acknowledgements

We thank Dr. Guillermo Oliver and St. Jude Children's research hospital for generous support during the early stages of this work. We thank Drs. Rodger McEver and Lorin Olson for critical reading of the manuscript and for insightful comments, Dr. Ying Yang for vibratome sectioning and staining protocol, Mr. Michael McDaniel for help with confocal microscopy, Dr. Jane Song for data analysis using ImageJ and GraphPad Prism, Dr. Pierre Chambon for CreERT2 cDNA, Ms. Lisa Whitworth (Microscopy Laboratory, Oklahoma State University, Stillwater) for SEM and Pickersgill & Andersen, Life Science Editors, for editorial assistance. RSS is supported by institutional funds of OMRF, Oklahoma Center for Adult Stem Cell Research (OCASCR, 4340), American Heart Association (15BGIA25710032) and NIH/NIGMS COBRE (P20 GM103441 PI: Dr. McEver).

References

Adams RH, Alitalo K. Molecular regulation of angiogenesis and lymphangiogenesis. Nature reviews Molecular cell biology. 2007; 8:464–478. [PubMed: 17522591]

Armstrong EJ, Bischoff J. Heart valve development: endothelial cell signaling and differentiation. Circulation research. 2004; 95:459–470. [PubMed: 15345668]

Armulik A, Genove G, Betsholtz C. Pericytes: developmental, physiological, and pathological perspectives, problems, and promises. Developmental cell. 2011; 21:193–215. [PubMed: 21839917]

Bazigou E, Lyons OT, Smith A, Venn GE, Cope C, Brown NA, Makinen T. Genes regulating lymphangiogenesis control venous valve formation and maintenance in mice. The Journal of clinical investigation. 2011; 121:2984–2992. [PubMed: 21765212]

Bazigou E, Xie S, Chen C, Weston A, Miura N, Sorokin L, Adams R, Muro AF, Sheppard D, Makinen T. Integrin-alpha9 is required for fibronectin matrix assembly during lymphatic valve morphogenesis. Developmental cell. 2009; 17:175–186. [PubMed: 19686679]

Bertozzi CC, Schmaier AA, Mericko P, Hess PR, Zou Z, Chen M, Chen CY, Xu B, Lu MM, Zhou D, et al. Platelets regulate lymphatic vascular development through CLEC-2-SLP-76 signaling. Blood. 2010; 116:661–670. [PubMed: 20363774]

Bowles J, Secker G, Nguyen C, Kazenwadel J, Truong V, Frampton E, Curtis C, Skoczylas R, Davidson TL, Miura N, et al. Control of retinoid levels by CYP26B1 is important for lymphatic vascular development in the mouse embryo. Developmental biology. 2014; 386:25–33. [PubMed: 24361262]

Chang CP, Neilson JR, Bayle JH, Gestwicki JE, Kuo A, Stankunas K, Graef IA, Crabtree GR. A field of myocardial-endocardial NFAT signaling underlies heart valve morphogenesis. Cell. 2004; 118:649–663. [PubMed: 15339668]

Chen H, Griffin C, Xia L, Srinivasan RS. Molecular and cellular mechanisms of lymphatic vascular maturation. Microvascular research. 2014; 96:16–22. [PubMed: 24928499]

Coxam B, Sabine A, Bower NI, Smith KA, Pichol-Thievend C, Skoczylas R, Astin JW, Frampton E, Jaquet M, Crosier PS, et al. Pkd1 regulates lymphatic vascular morphogenesis during development. Cell reports. 2014; 7:623–633. [PubMed: 24767999]

Francois M, Caprini A, Hosking B, Orsenigo F, Wilhelm D, Browne C, Paavonen K, Karnezis T, Shayan R, Downes M, et al. Sox18 induces development of the lymphatic vasculature in mice. Nature. 2008; 456:643–647. [PubMed: 18931657]

Francois M, Short K, Secker GA, Combes A, Schwarz Q, Davidson TL, Smyth I, Hong YK, Harvey NL, Koopman P. Segmental territories along the cardinal veins generate lymph sacs via a ballooning mechanism during embryonic lymphangiogenesis in mice. Developmental biology. 2012; 364:89–98. [PubMed: 22230615]

Fu J, Gerhardt H, McDaniel JM, Xia B, Liu X, Ivanciu L, Ny A, Hermans K, Silasi-Mansat R, McGee S, et al. Endothelial cell O-glycan deficiency causes blood/lymphatic misconnections and consequent fatty liver disease in mice. The Journal of clinical investigation. 2008; 118:3725–3737. [PubMed: 18924607]

Furumoto TA, Miura N, Akasaka T, Mizutani-Koseki Y, Sudo H, Fukuda K, Maekawa M, Yuasa S, Fu Y, Moriya H, et al. Notochord-dependent expression of MFH1 and PAX1 cooperates to maintain the proliferation of sclerotome cells during the vertebral column development. Developmental biology. 1999; 210:15–29. [PubMed: 10364424]

Hagerling R, Pollmann C, Kremer L, Andresen V, Kiefer F. Intravital two-photon microscopy of lymphatic vessel development and function using a transgenic Prox1 promoter-directed mOrange2 reporter mouse. Biochemical Society transactions. 2011; 39:1674–1681. [PubMed: 22103506]

Hess PR, Rawnsley DR, Jakus Z, Yang Y, Sweet DT, Fu J, Herzog B, Lu M, Nieswandt B, Oliver G, et al. Platelets mediate lymphovenous hemostasis to maintain blood-lymphatic separation throughout life. The Journal of clinical investigation. 2014; 124:273–284. [PubMed: 24292710]

Hong YK, Harvey N, Noh YH, Schacht V, Hirakawa S, Detmar M, Oliver G. Prox1 is a master control gene in the program specifying lymphatic endothelial cell fate. Developmental dynamics : an official publication of the American Association of Anatomists. 2002; 225:351–357. [PubMed: 12412020]

Iida K, Koseki H, Kakinuma H, Kato N, Mizutani-Koseki Y, Ohuchi H, Yoshioka H, Noji S, Kawamura K, Kataoka Y, et al. Essential roles of the winged helix transcription factor MFH-1 in aortic arch patterning and skeletogenesis. Development. 1997; 124:4627–4638. [PubMed: 9409679]

Kanady JD, Dellinger MT, Munger SJ, Witte MH, Simon AM. Connexin37 and Connexin43 deficiencies in mice disrupt lymphatic valve development and result in lymphatic disorders including lymphedema and chylothorax. Developmental biology. 2011; 354:253–266. [PubMed: 21515254]

Karkkainen MJ, Haiko P, Sainio K, Partanen J, Taipale J, Petrova TV, Jeltsch M, Jackson DG, Talikka M, Rauvala H, et al. Vascular endothelial growth 36 factor C is required for sprouting of the first lymphatic vessels from embryonic veins. Nature immunology. 2004; 5:74–80. [PubMed: 14634646]

Kazenwadel J, Betterman KL, Chong CE, Stokes PH, Lee YK, Secker GA, Agalarov Y, Demir CS, Lawrence DM, Sutton DL, et al. GATA2 is required for lymphatic vessel valve development and maintenance. The Journal of clinical investigation. 2015

Kazenwadel J, Secker GA, Liu YJ, Rosenfeld JA, Wildin RS, Cuellar-Rodriguez J, Hsu AP, Dyack S, Fernandez CV, Chong CE, et al. Loss-of-function germline GATA2 mutations in patients with MDS/AML or MonoMAC syndrome and primary lymphedema reveal a key role for GATA2 in the lymphatic vasculature. Blood. 2012; 119:1283–1291. [PubMed: 22147895]

Khandekar M, Brandt W, Zhou Y, Dagenais S, Glover TW, Suzuki N, Shimizu R, Yamamoto M, Lim KC, Engel JD. A Gata2 intronic enhancer confers its pan-endothelia-specific regulation. Development. 2007; 134:1703–1712. [PubMed: 17395646]

Klein KR, Karpinich NO, Espenschied ST, Willcockson HH, Dunworth WP, Hoopes SL, Kushner EJ, Bautch VL, Caron KM. Decoy receptor CXCR7 modulates adrenomedullin-mediated cardiac and lymphatic vascular development. Developmental cell. 2014; 30:528–540. [PubMed: 25203207]

Lim KC, Hosoya T, Brandt W, Ku CJ, Hosoya-Ohmura S, Camper SA, Yamamoto M, Engel JD. Conditional Gata2 inactivation results in HSC loss and lymphatic mispatterning. The Journal of clinical investigation. 2012; 122:3705–3717. [PubMed: 22996665]

Majesky MW, Dong XR, Regan JN, Hoglund VJ. Vascular smooth muscle progenitor cells: building and repairing blood vessels. Circulation research. 2011; 108:365–377. [PubMed: 21293008]

Makinen T, Adams RH, Bailey J, Lu Q, Ziemiecki A, Alitalo K, Klein R, Wilkinson GA. PDZ interaction site in ephrinB2 is required for the remodeling of lymphatic vasculature. Genes & development. 2005; 19:397–410. [PubMed: 15687262]

Munger SJ, Kanady JD, Simon AM. Absence of venous valves in mice lacking Connexin37. Developmental biology. 2013; 373:338–348. [PubMed: 23142761]

Norrmen C, Ivanov KI, Cheng J, Zangger N, Delorenzi M, Jaquet M, Miura N, Puolakkainen P, Horsley V, Hu J, et al. FOXC2 controls formation and maturation of lymphatic collecting vessels through cooperation with NFATc1. The Journal of cell biology. 2009; 185:439–457. [PubMed: 19398761]

Ostergaard P, Simpson MA, Connell FC, Steward CG, Brice G, Woollard WJ, Dafou D, Kilo T, Smithson S, Lunt P, et al. Mutations in GATA2 cause primary lymphedema associated with a predisposition to acute myeloid leukemia (Emberger syndrome). Nature genetics. 2011; 43:929–931. [PubMed: 21892158]

Outeda P, Huso DL, Fisher SA, Halushka MK, Kim H, Qian F, Germino GG, Watnick T. Polycystin signaling is required for directed endothelial cell migration and lymphatic development. Cell reports. 2014; 7:634–644. [PubMed: 24767998]

Petrova TV, Karpanen T, Norrmen C, Mellor R, Tamakoshi T, Finegold D, Ferrell R, Kerjaschki D, Mortimer P, Yla-Herttuala S, et al. Defective valves and abnormal mural cell recruitment underlie lymphatic vascular failure in lymphedema distichiasis. Nature medicine. 2004; 10:974–981.

Petrova TV, Makinen T, Makela TP, Saarela J, Virtanen I, Ferrell RE, Finegold DN, Kerjaschki D, Yla-Herttuala S, Alitalo K. Lymphatic endothelial 38 reprogramming of vascular endothelial cells by the Prox-1 homeobox transcription factor. The EMBO journal. 2002; 21:4593–4599. [PubMed: 12198161]

Phan SH. The myofibroblast in pulmonary fibrosis. Chest. 2002; 122:286S–289S. [PubMed: 12475801]

Potapova TA, Sivakumar S, Flynn JN, Li R, Gorbsky GJ. Mitotic progression becomes irreversible in prometaphase and collapses when Wee1 and Cdc25 are inhibited. Molecular biology of the cell. 2011; 22:1191–1206. [PubMed: 21325631]

Raymond CS, Soriano P. High-efficiency FLP and PhiC31 site-specific recombination in mammalian cells. PloS one. 2007; 2:e162. [PubMed: 17225864]

Sabine A, Agalarov Y, Maby-El Hajjami H, Jaquet M, Hagerling R, Pollmann C, Bebber D, Pfenniger A, Miura N, Dormond O, et al. Mechanotransduction, PROX1, and FOXC2 cooperate to control connexin37 and calcineurin during lymphaticvalve formation. Developmental cell. 2012; 22:430–445. [PubMed: 22306086]

Seeger M, Bewig B, Gunther R, Schafmayer C, Vollnberg B, Rubin D, Hoell C, Schreiber S, Folsch UR, Hampe J. Terminal part of thoracic duct: highresolution US imaging. Radiology. 2009; 252:897–904. [PubMed: 19703864]

Seo S, Kume T. Forkhead transcription factors, Foxc1 and Foxc2, are required for the morphogenesis of the cardiac outflow tract. Developmental biology. 2006; 296:421–436. [PubMed: 16839542]

Simon AM, Goodenough DA, Li E, Paul DL. Female infertility in mice lacking connexin 37. Nature. 1997; 385:525–529. [PubMed: 9020357]

Srinivasan RS, Dillard ME, Lagutin OV, Lin FJ, Tsai S, Tsai MJ, Samokhvalov IM, Oliver G. Lineage tracing demonstrates the venous origin of the mammalian lymphatic vasculature. Genes & development. 2007; 21:2422–2432. [PubMed: 17908929]

Srinivasan RS, Escobedo N, Yang Y, Interiano A, Dillard ME, Finkelstein D, Mukatira S, Gil HJ, Nurmi H, Alitalo K, et al. The Prox1-Vegfr3 feedback loop maintains the identity and the number

of lymphatic endothelial cell progenitors. Genes & development. 2014; 28:2175–2187. [PubMed: 25274728]

Srinivasan RS, Geng X, Yang Y, Wang Y, Mukatira S, Studer M, Porto MP, Lagutin O, Oliver G. The nuclear hormone receptor Coup-TFII is required for the initiation and early maintenance of Prox1 expression in lymphatic endothelial cells. Genes & development. 2010; 24:696–707. [PubMed: 20360386]

Srinivasan RS, Oliver G. Prox1 dosage controls the number of lymphatic endothelial cell progenitors and the formation of the lymphovenous valves. Genes & development. 2011; 25:2187–2197. [PubMed: 22012621]

Tammela T, Alitalo K. Lymphangiogenesis: Molecular mechanisms and future promise. Cell. 2010; 140:460–476. [PubMed: 20178740]

Tatin F, Taddei A, Weston A, Fuchs E, Devenport D, Tissir F, Makinen T. Planar cell polarity protein Celsr1 regulates endothelial adherens junctions and directed cell rearrangements during valve morphogenesis. Developmental cell. 2013; 26:31–44. [PubMed: 23792146]

Truman LA, Bentley KL, Smith EC, Massaro SA, Gonzalez DG, Haberman AM, Hill M, Jones D, Min W, Krause DS, et al. ProxTom lymphatic vessel reporter mice reveal Prox1 expression in the adrenal medulla, megakaryocytes, and platelets. The American journal of pathology. 2012; 180:1715–1725. [PubMed: 22310467]

Tsai FY, Keller G, Kuo FC, Weiss M, Chen J, Rosenblatt M, Alt FW, Orkin SH. An early haematopoietic defect in mice lacking the transcription factor GATA-2. Nature. 1994; 371:221–226. [PubMed: 8078582]

Turner CJ, Badu-Nkansah K, Crowley D, van der Flier A, Hynes RO. Integrinalpha5beta1 is not required for mural cell functions during development of blood vessels but is required for lymphatic-blood vessel separation and lymphovenous valve formation. Developmental biology. 2014; 392:381–392. [PubMed: 24858485]

Uhrin P, Zaujec J, Breuss JM, Olcaydu D, Chrenek P, Stockinger H, Fuertbauer E, Moser M, Haiko P, Fassler R, et al. Novel function for blood platelets and podoplanin in developmental separation of blood and lymphatic circulation. Blood. 2010; 115:3997–4005. [PubMed: 20110424]

Wigle JT, Oliver G. Prox1 function is required for the development of the murine lymphatic system. Cell. 1999; 98:769–778. [PubMed: 10499794]

Yang Y, Garcia-Verdugo JM, Soriano-Navarro M, Srinivasan RS, Scallan JP, Singh MK, Epstein JA, Oliver G. Lymphatic endothelial progenitors bud from the cardinal vein and intersomitic vessels in mammalian embryos. Blood. 2012; 120:2340–2348. [PubMed: 22859612]

Highlights

- Characterization of lymphovenous valve (LVV) morphogenesis at the molecular and ultrastructural levels.
- Newly formed LVV-forming endothelial cells (LVV-ECs) delaminate from the vein in the luminal direction.
- LVV-ECs reassemble, align perpendicular to fluid flow and establish lymphovenous connections.
- Maturation of LVVs involves the recruitment of mural cells.
- LVV defects are associated with lymphedema.

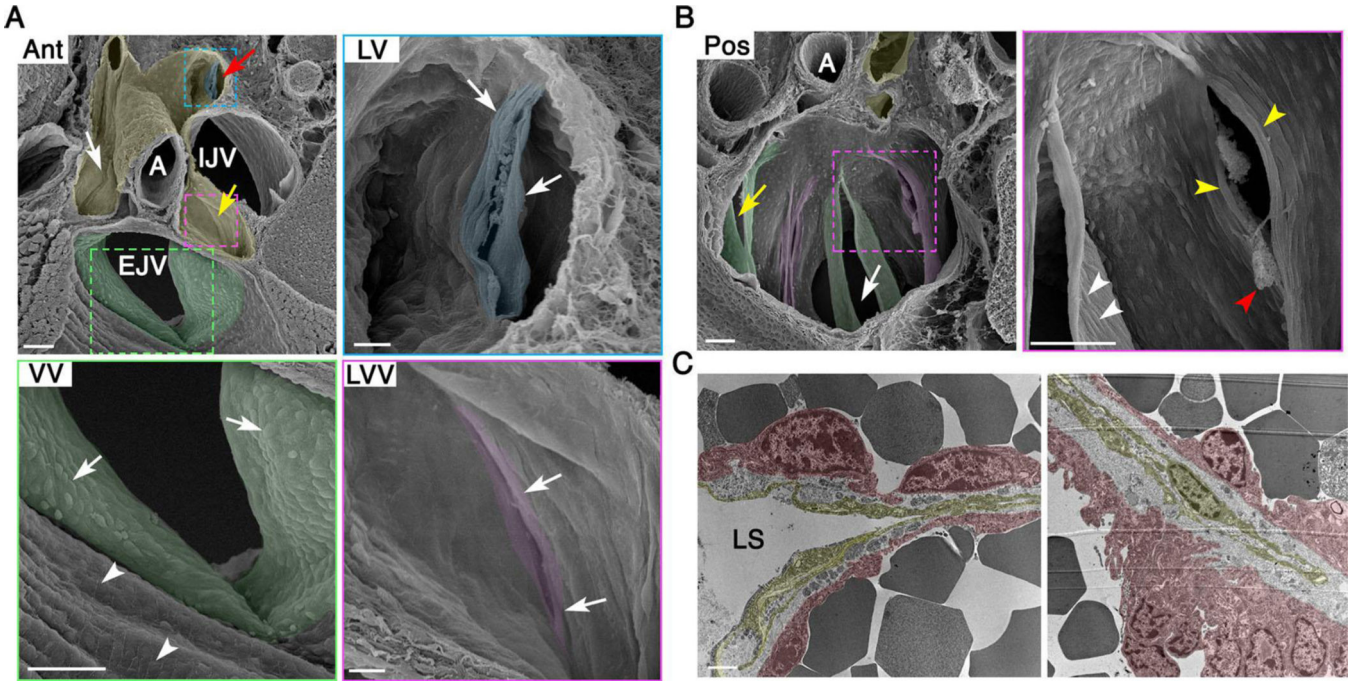

Figure 1. Organization of cells in the lymphovenous valve (LVV) complex of newborn mice

(A) SEM in the anterior-to-posterior (Ant) orientation shows lymph sac (pseudo colored in yellow), upstream sides of LVVs (white and yellow arrows), VV within EJV (pseudo colored in green) and the downstream side of a LV (pseudo colored in blue). At higher magnification, LVVs appear to have a smaller opening compared to VV. And, cells at the entrance of LVVs are elongated perpendicular to the direction lymph flow, which is away from the reader. Cells within EJV are seen aligned parallel to the direction of blood flow (VV, arrowheads). Instead, cells within VV are cuboidal (VV, arrows). (B) SEM in the posterior-to-anterior (Pos) orientation shows the downstream side of LVVs (magenta) and VVs (green). White arrow indicates EJV and yellow arrow indicates SCV. At higher magnification cells in both LVVs and VVs (yellow and white arrowheads respectively) appear elongated. Cells on the downstream side of LVs are also elongated (A, LV, arrows). Fibrin clots at the entrance of LVVs are also seen (red arrowhead). (C) TEM shows thin and elongated lymphatic endothelial cells in the upstream end of LVVs (yellow). LVV-forming endothelial cells on the veins are in magenta.

Statistics: n= 4 for A, B. n= 2 for C.

Abbreviations: LS, lymph sac; A, artery; IJV, internal jugular vein; EJV, external jugular vein; SCV, subclavian vein; SVC, superior vena cava.

Scale bars: 50 μm for A (Ant, VV) and B; 10 μm for A (LVV, LV) and 1 μm for C.

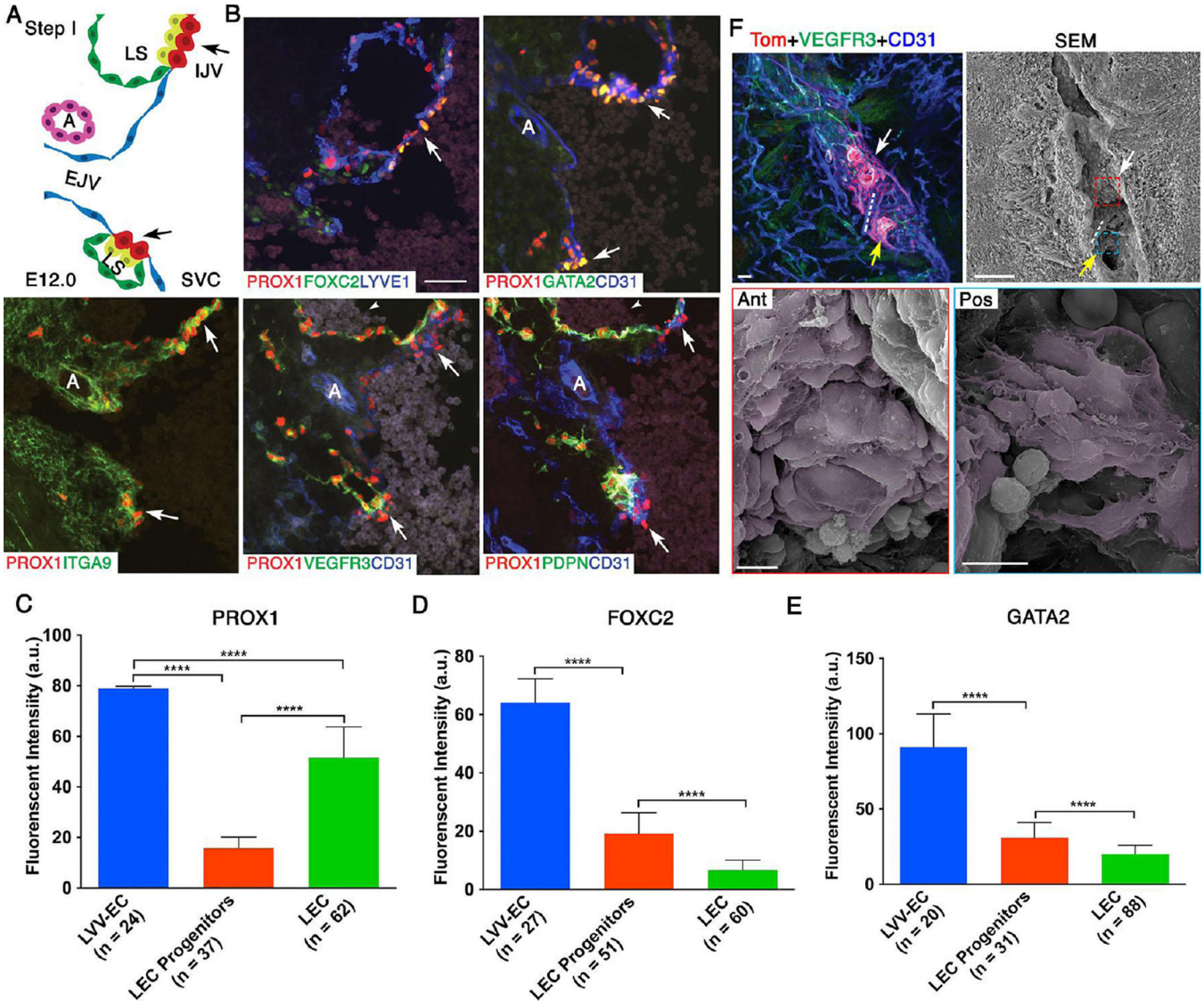

Figure 2. At E12.0 LVV-forming endothelial cells (LVV-ECs) delaminate from the veins in the luminal orientation

(A) Organization of veins and lymph sacs (LS) in the frontal orientation at this first step of LVV development. Lymphatic endothelial cells (LECs) and LVV-ECs that form LVVs are in yellow and red respectively. The remaining LECs that form LS and venous endothelial cells are in green and blue respectively. EJV is perpendicular to IJV and SVC. (B) Immunohistochemistry for the indicated markers in the region from panel A. LVV-ECs are indicated by arrows. PROX1 is expressed at higher level in LVV-ECs compared to LECs. FOXC2 and GATA2 are expressed almost exclusively in LVV-ECs. In contrast, PDPN is restricted to LECs. VEGFR3 is higher in LVV forming LECs compared to LVV-ECs and the rest of LECs. ITGA9 is strongly expressed in the LVV forming LECs and LVV-ECs. Arrowheads point to the blood cells seen within the lymph sacs. (C-E) After performing immunohistochemistry on sections as described above, the fluorescent signals produced by antibodies were measured in arbitrary units (a.u.) using ImageJ software. PROX1 (C), FOXC2 (D) and GATA2 (E) are expressed at significantly higher levels in LVV-ECs

compared to LEC progenitors and LECs. (F) 800 μm sagittal section of an E12.0 ProxTom embryo was immunostained and imaged by confocal microscopy. Two loose clusters of Tom^{high} LVV-ECs are seen within the vein. Dotted line represents the artery located between the LVV-ECs clusters. SEM of the same section revealed delaminating LVV-ECs that overlap each other (pseudo colored in magenta) in both anterior (white arrow) and posterior (yellow arrow) clusters.

Statistics: n= 3 for B; n= 6 for F. For panels C-E, the indicated numbers of cells from a single embryo were analyzed. This data is representative of three-independent experiments. **** $p<0.0001$.

Abbreviations: LS, lymph sac; IJV, internal jugular vein; EJV, external jugular vein; SCV, subclavian vein; SVC, superior vena cava.

Scale bars: 50 μm for B and the top two panels of C; 10 μm for the bottom two panels of C.

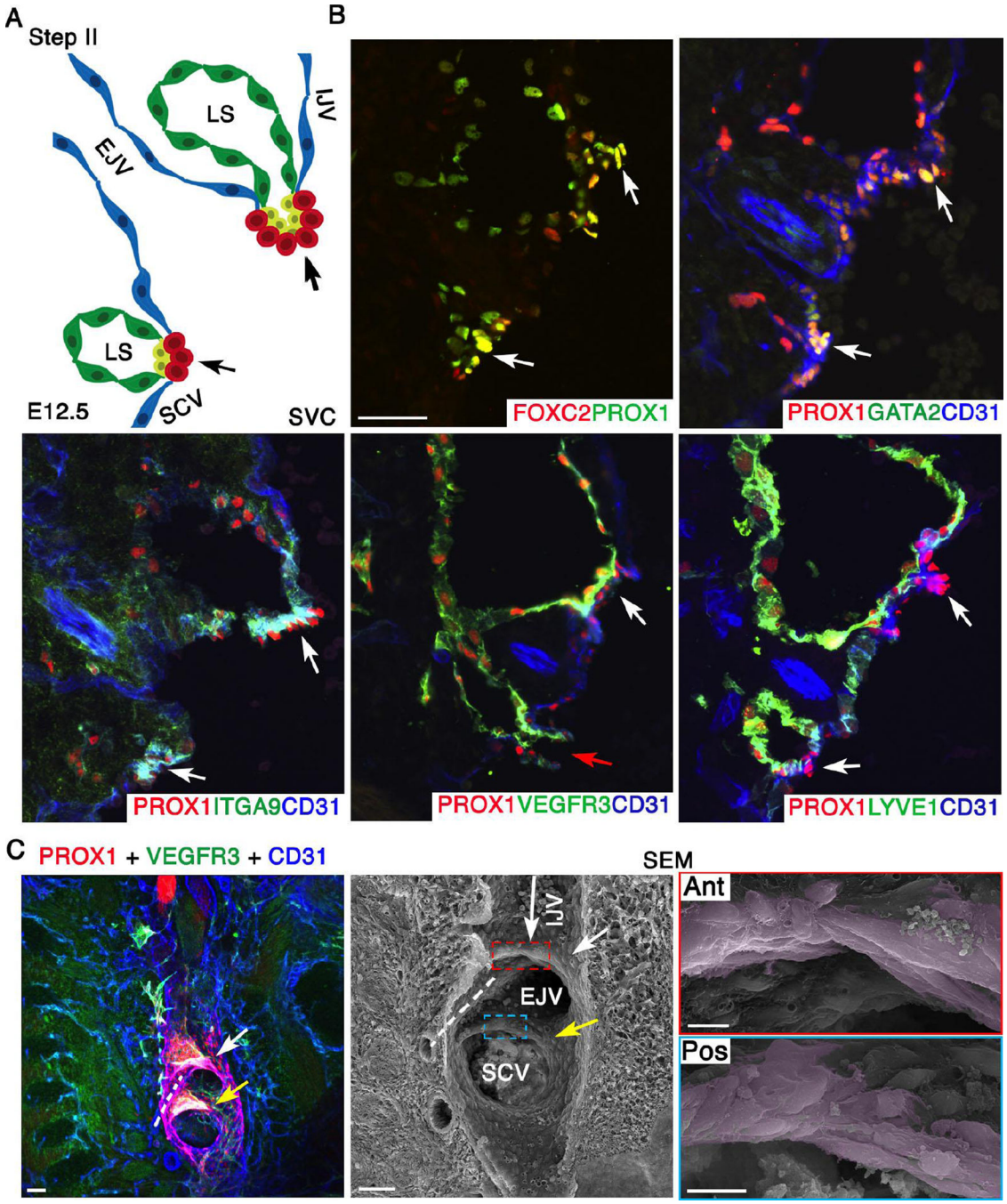

Figure 3. At E12.5 LVV-EC clusters invaginate into the veins and elongate perpendicular to blood flow

(A) Schematic of the LVV complex in frontal orientation at E12.5. This is the second step of LVV development. Cells are color coded as in Figure 2. Note that the EJV has rotated clockwise towards IJV by 45°. (B) Immunohistochemistry revealed that the LVV-ECs (white arrows) have invaginated into the veins. And, a connection between LS and veins is seen (red arrow). LYVE1 is excluded from LVV-ECs at E12.5. Expression pattern of other markers is identical to that at E12.0. (C) Confocal imaging followed by SEM of an 800 μm sagittal section from a E12.5 ProxTom embryo revealed two compact Tom^{high} LVV-EC

clusters. Cells in both anterior (white arrow) and posterior (yellow arrow) clusters have elongated perpendicular to the direction of blood flow. The long arrow indicates the direction of flow in IJV. The flow from EJV and SCV are towards the reader. Dotted line indicates the artery between the two LVVs.

Statistics: n= 3 for B. n= 8 for C.

Abbreviations: LS, lymph sac; IJV, internal jugular vein; EJV, external jugular vein; SCV, subclavian vein; SVC, superior vena cava.

Scale bars: 50 μm for B and the first two panels of C; 10 μm for the last two panels of C.

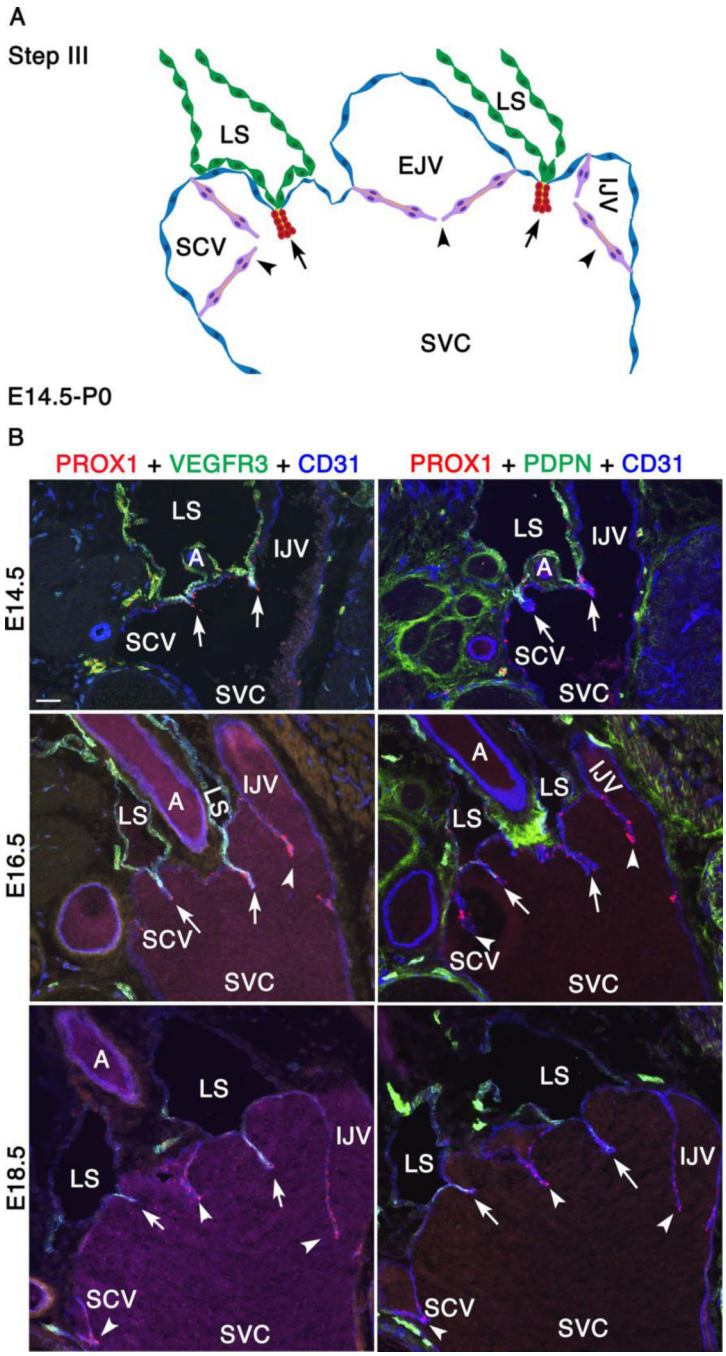

Figure 4. Between E14.5 and P0, VVs are formed and LEC markers are gradually downregulated in lymph sacs

(A) This is the third and final step of LVV development between E14.5 and P0. The schematic depicts the overall arrangement of the LVV complex in frontal orientation. The only obvious change during this interval is the appearance of VVs at E16.5. VVs are in magenta. Rest of the cells is color coded as in Figure 2. (B) Immunohistochemistry revealed that the LEC markers VEGFR3 and podoplanin (PDPN) are gradually downregulated in LSs. However, they remain strongly expressed in the LECs that form LVVs (arrows). Statistics: n= 3 for each developmental stage.

Abbreviations: LS, lymph sac; IJV, internal jugular vein; EJV, external jugular vein; SCV, subclavian vein; SVC, superior vena cava.
Scale bars: 50 μm for B and 1 μm for C.

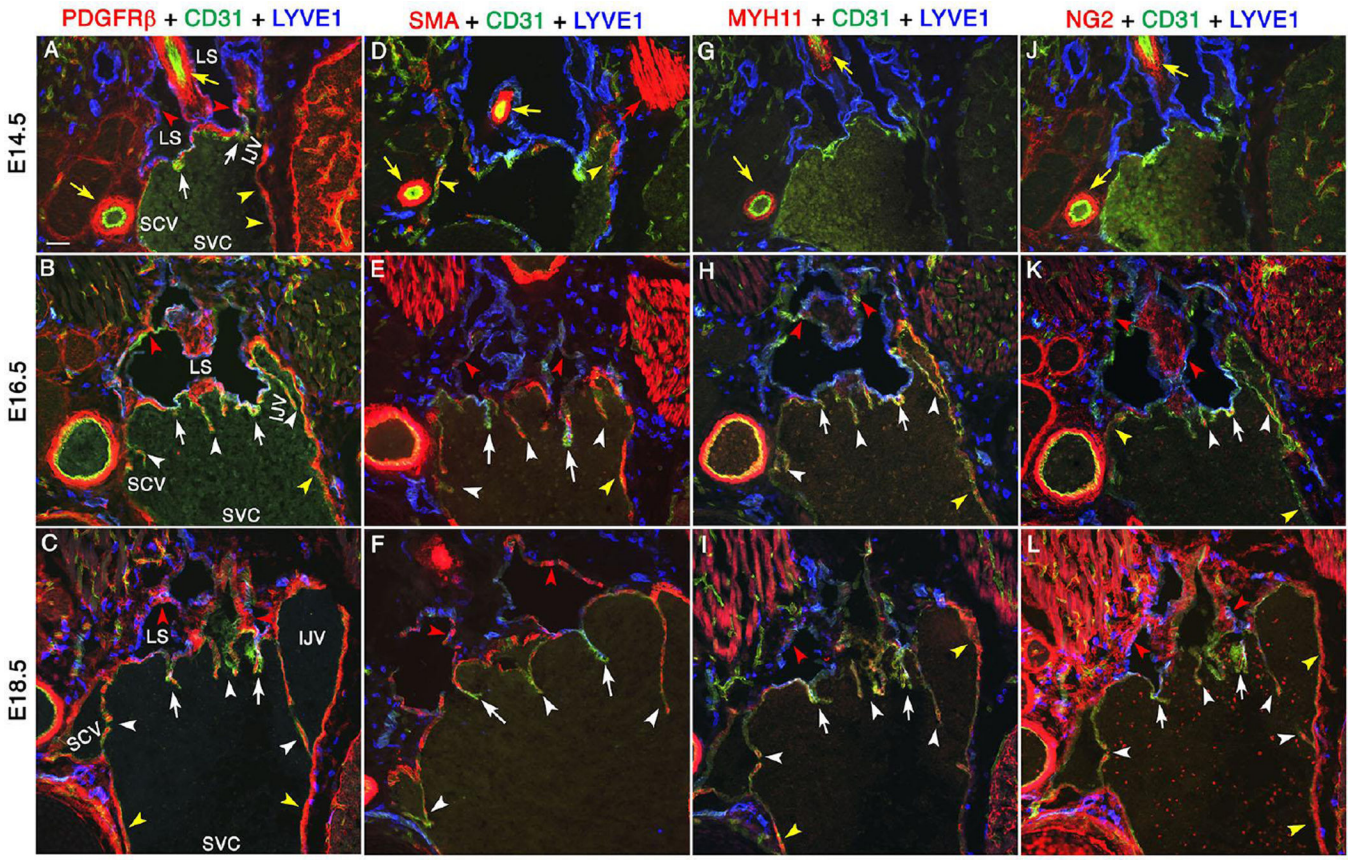

Figure 5. Mural cells are progressively recruited to lymph sacs, LVVs and VVs

Mural cells are progressively recruited to lymph sacs, LVVs and VVs. LVV-forming region of E14.5, E16.5 and E18.5 embryos were analyzed using mural cell markers. PDGFRβ (A-C) is a pan-mural cell marker. SMA (D-F) and MYH11 (G-I) are vascular smooth muscle cell markers. NG2 is a pericyte marker (J-L). At E14.5, PDGFRβ^{+} cells are is seen surrounding the lymph sacs (A, red arrowheads) and within LVVs (A, white arrows). Other mural cell markers are not seen in lymph sacs or LVVs at this stage (D, G, J). At subsequent developmental time points, downregulation of LEC marker LYVE1 in lymph sacs coincides with the expression of mature mural cell markers (red arrowheads). Scattered mural cells are also seen within LVVs (white arrows) and VVs (white arrowheads). Yellow arrows and yellow arrowheads point to the arterial and venous perivascular cells respectively. And, red arrows point to the muscles.

Statistics: *n*= 3 for each developmental stage.

Abbreviations: LS, lymph sac; IJV, internal jugular vein; EJV, external jugular vein; SCV, subclavian vein; SVC, superior vena cava.

Scale bars: 50 μm

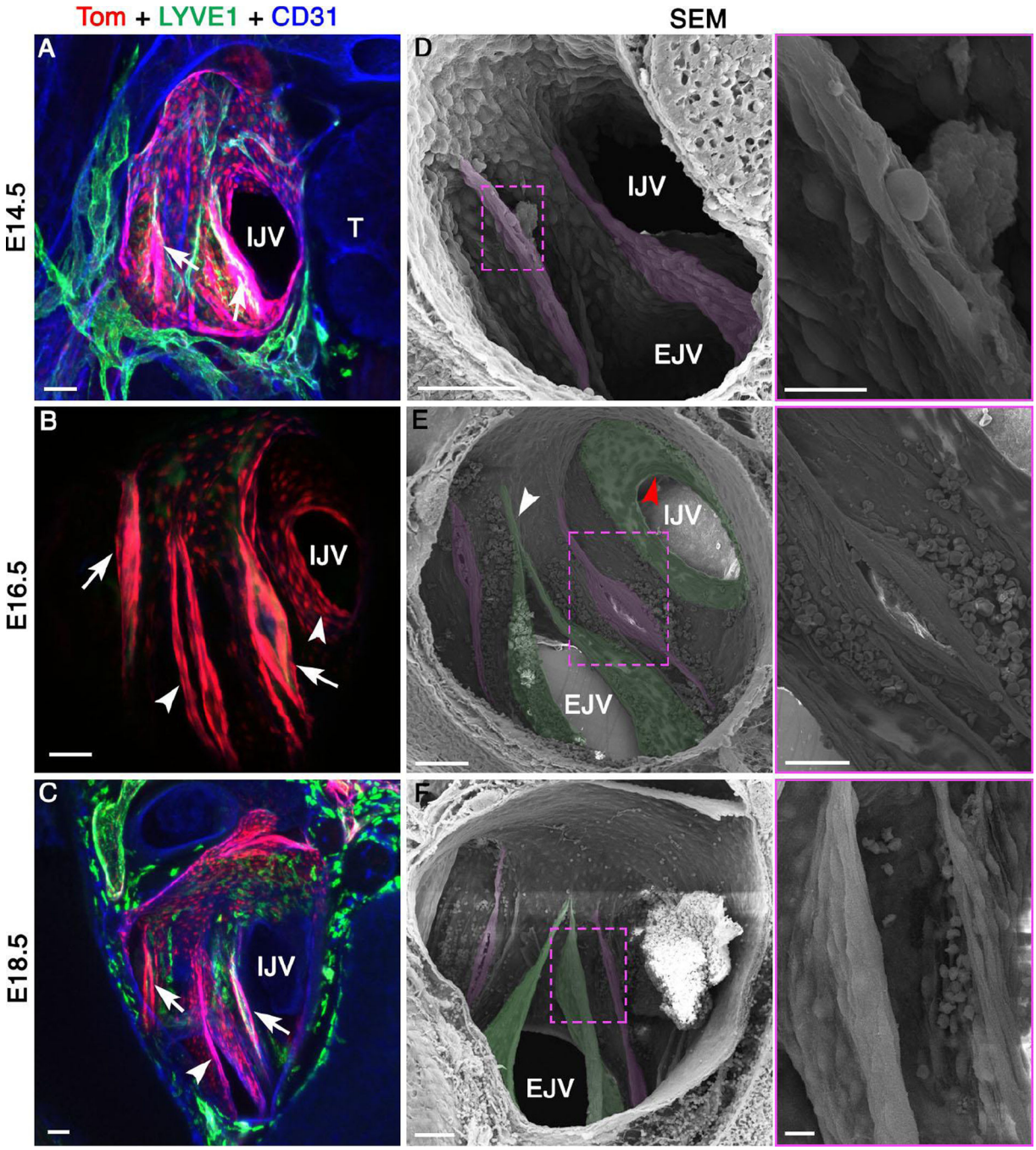

Figure 6. LVV-ECs undergo limited change while VVs rapidly develop between E14.5 and E18.5

(A-C) Confocal imaging of LVV-complex from ProxTom embryos in the Pos orientation reveals LVVs (arrows). VVs are seen at E16.5 and E18.5 (arrowheads). (D-F) SEM of the same samples reveals LVVs (pseudo colored in magenta) and VVs (pseudo colored in green). Higher magnification picture of the boxed areas are shown in the adjacent panels. The overall structure of LVVs remains stable in this time window. LVV-ECs appear to become more elongated with time. Diameter of venous junction increases during this time period. (D) VVs are not seen at E14.5. (E) At E16.5 VV at the entrance of IJV appears as a

circular shelf (stage 2 according to the scheme of Bazigou et al., 2011). A commissure is clearly seen in the VV located in EJV (arrowhead) suggesting developmental stage 3. (F) At E18.5 VV of EJV is dome shaped and fully matured (stage 4).
Statistics: n= 10 for A, D; n= 12 for B, E; n= 3 for C, F.
Abbreviations: T, thymus; IJV, internal jugular vein; EJV, external jugular vein.
Scale bars: 10 μm for E, G and I. 50 μm for the rest.

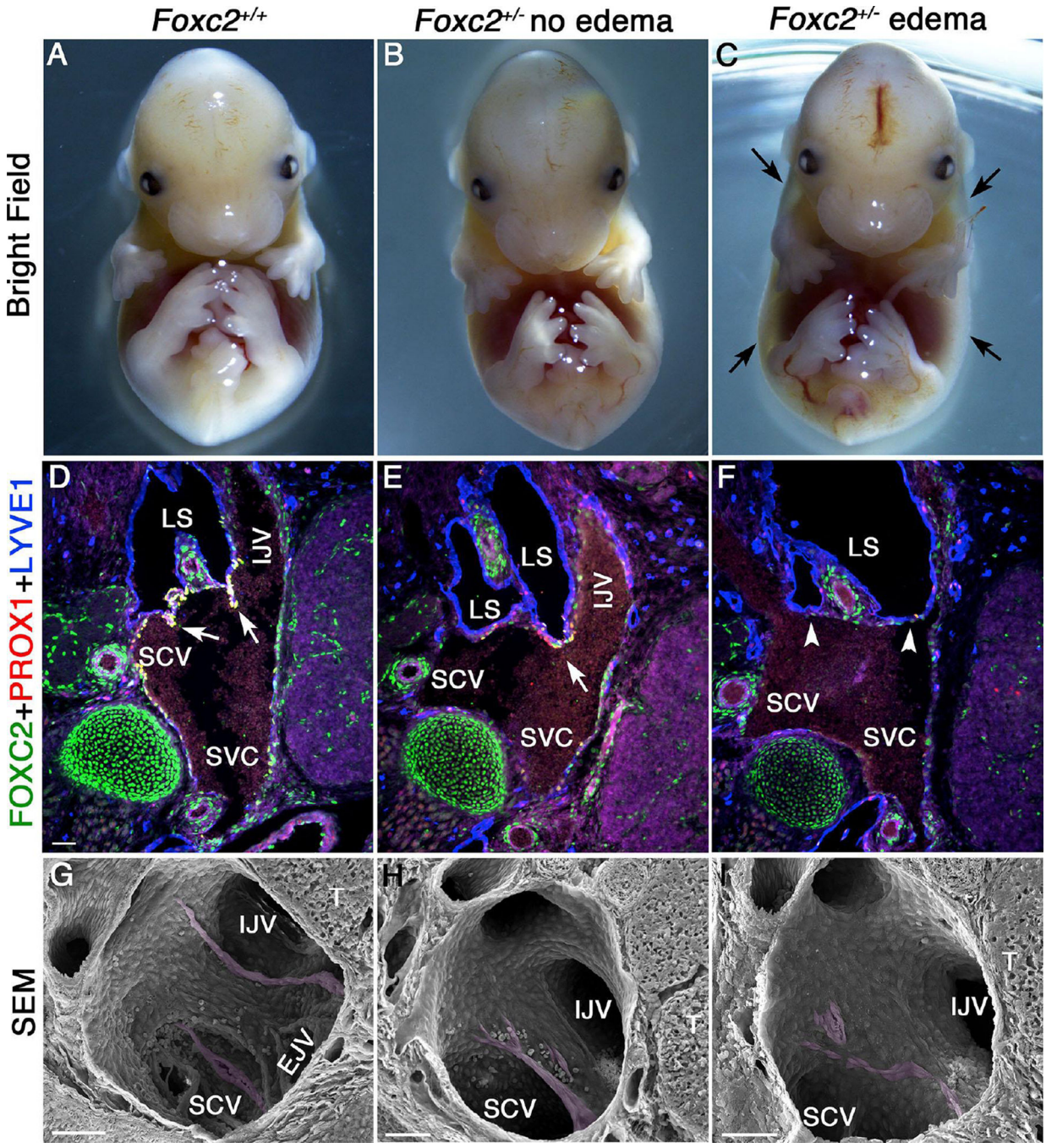

Figure 7. Variable penetrance of edema phenotype in Foxc2$^{+/-}$ embryos correlates with defective LVVs

Approximately half of the Foxc2-heterozygoes embryos generated in C57BL/6 background are grossly indistinguishable from wild type embryos (A, B). The other half develops edema (C, arrows) by E14.5. Analysis of frontal sections from these embryos revealed one LVV in the normal-looking Foxc2$^{+/-}$ embryos (E, arrow). The edematous embryos lack LVVs (F, arrowheads). (G-I) SEM of the LVV-complex from control embryos revealed two LVVs (G, magenta) in control and one LVV (H, magenta) in non-edematous Foxc2-heterozygote

embryos. In contrast, no LVVs are seen in edematous Foxc2-heterozygoes (I). Instead, a few elongated cells with the characteristics of LVV-ECs are seen (magenta).

Statistics: n= 3 for A-G; n = 4 for H; n = 2 for I.

Abbreviations: SVC, superior vena cava; SCV, subclavian vein; LS, lymph sac; IJV, internal jugular vein.

Scale bars: 50 μm

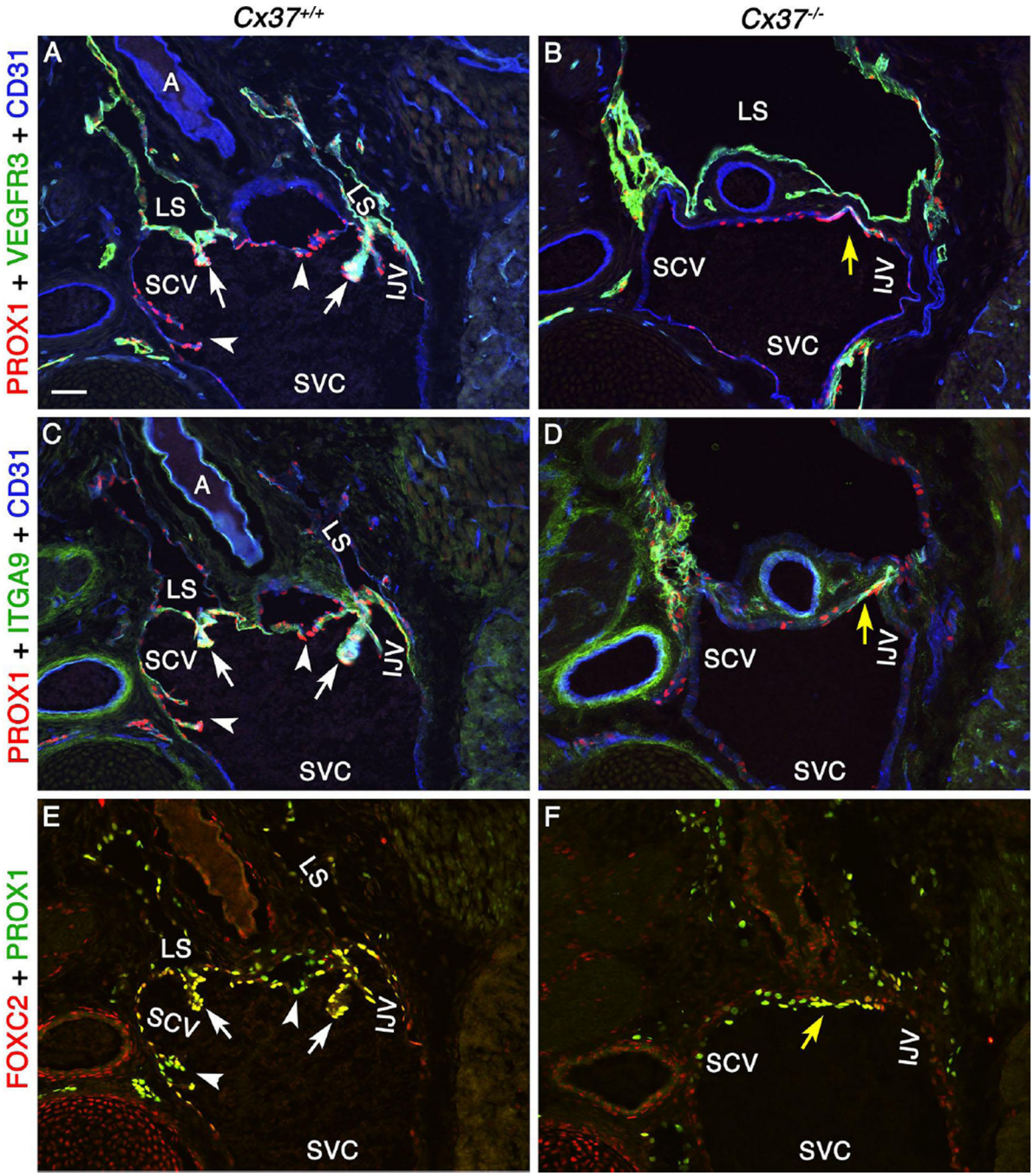

Figure 8. LVV-EC invagination is defective in Cx37$^{-/-}$ embryos

(A-F) E16.5 Cx37$^{+/+}$ and Cx37$^{-/-}$ embryos were sectioned and analyzed after immunostaining for the indicated markers. LVVs (arrows) and VVs (arrowheads) are seen in Cx37$^{+/+}$ embryos. LVV-ECs are observed in the valve-forming region of Cx37$^{-/-}$ embryos (yellow arrows) but they do not invaginate into veins to form clear LVVs or VVs.

Statistics: n= 2 for A, C and E; n = 4 for B, D and F.

Abbreviations: A, artery; LS, lymph sac; IJV, internal jugular vein; EJV, external jugular vein; SCV, subclavian vein; SVC, superior vena cava.

Scale bars: 50 μm

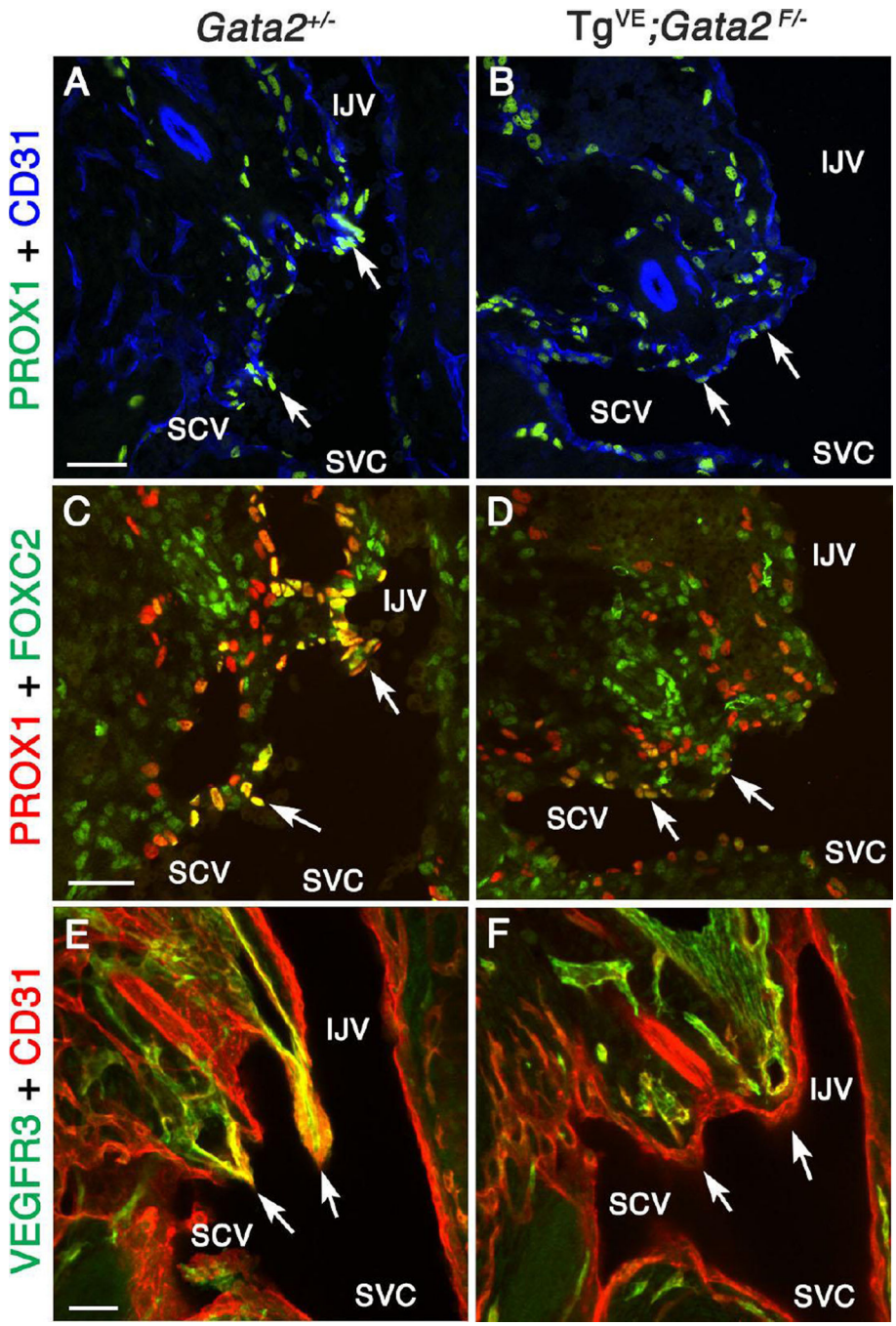

Figure 9. GATA2 is necessary for the proper differentiation of LVV-ECs

(A-F) E13.5 Gata2$^{+/-}$ or Tg^{VE};Gata2$^{f/-}$ (in which Gata2 is conditionally deleted from all endothelial cells using CreERT2 after tamoxifen injection at E10.0) embryos were analyzed using the indicated markers. A-D are 12 μm frontal cryosections. PROX1 (A, C arrows) and FOXC2 (C, arrows) are strongly expressed in LVV-ECs of Gata2$^{+/-}$ embryos. In contrast, PROX1 (B, D arrows) and FOXC2 (D, arrows) are weakly expressed in the LVV-forming region of Tg^{VE};Gata2$^{f/-}$ embryos. E and F are projections of 100 μm thick frontal

cryosections imaged by confocal microscopy. LVVs (E, arrows) seen in $Gata2^{+/-}$ are absent in Tg^{VE};$Gata2^{f/-}$ embryos (F, arrows).

Statistics: n= 3.

Abbreviations: LS, lymph sac; IJV, internal jugular vein; SCV, subclavian vein; SVC, superior vena cava.

Scale bars: 50 μm.

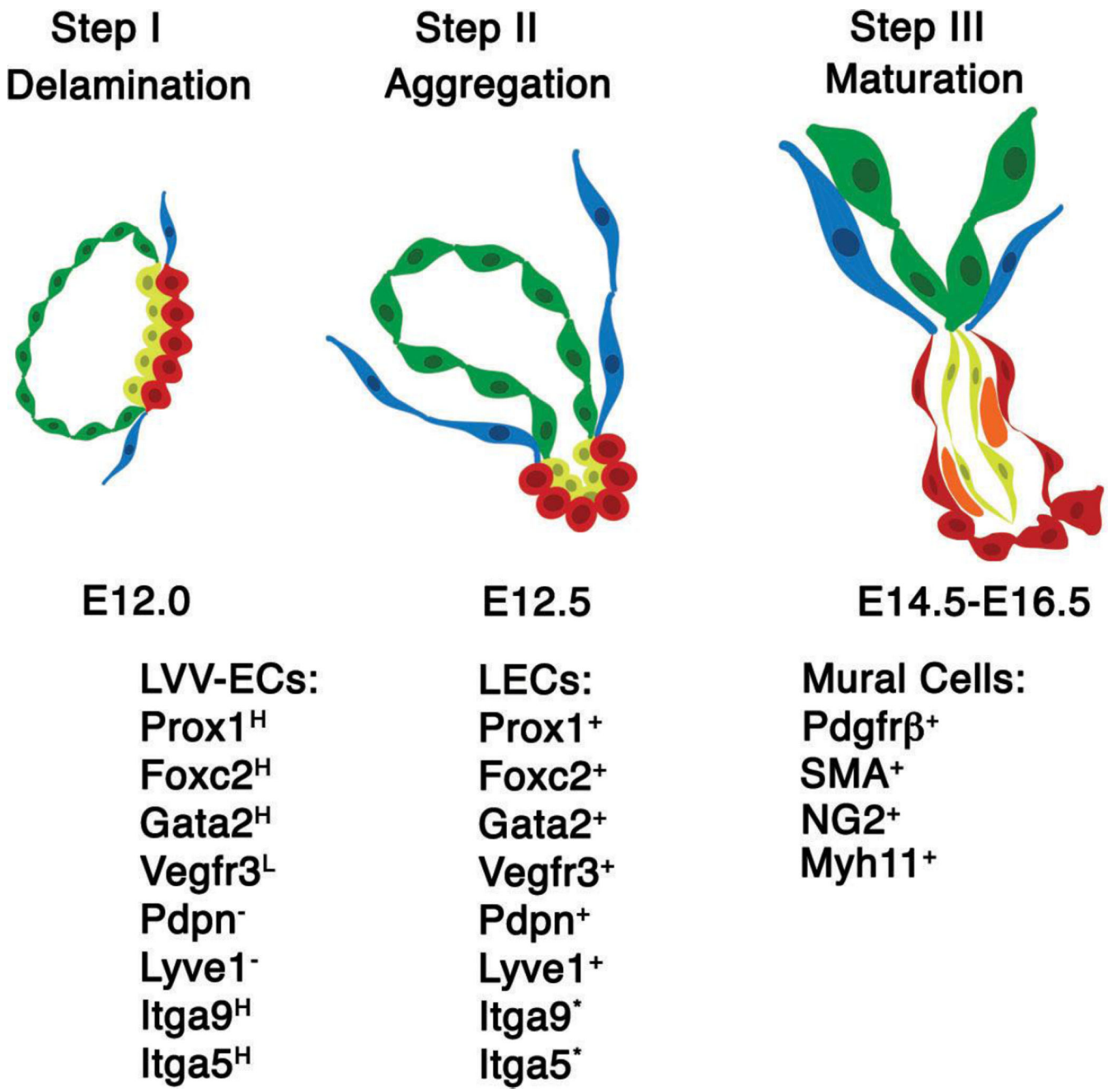

Figure 10. Summary of the morphological, cellular and molecular mechanisms controlling LVV morphogenesis

LVVs morphogenesis occurs in a stepwise manner. Step I: LVV-ECs (red) are specified from venous endothelial cells (blue). Step II: LVV-ECs and LECs (yellow) invaginate into the vein. Step III: Mural cells are recruited in between LECs and LVV-ECs. The expression pattern of various markers is indicated below the respective schematics.

Abbreviations: LVV-EC, LVV-forming endothelial cell; LECs, lymphatic endothelial cell; H-higher expression; L-lower expression; *-modest expression is observed in all LECs. However, expression appears to be enriched in the LECs that are juxtaposed to LVV-ECs.